Title
Prominent Postnatal Streams of Interneurons in the Ferret Cortex

Permalink
https://escholarship.org/uc/item/5zz9z4p0

Author
Ellis, Justin

Publication Date
2017

Peer reviewed|Thesis/dissertation

Prominent Postnatal Streams Of Interneurons In The Ferret Cortex

by

Justin Kyle Ellis, MD

DISSERTATION

Submitted in partial satisfaction of the requirements for the degree of
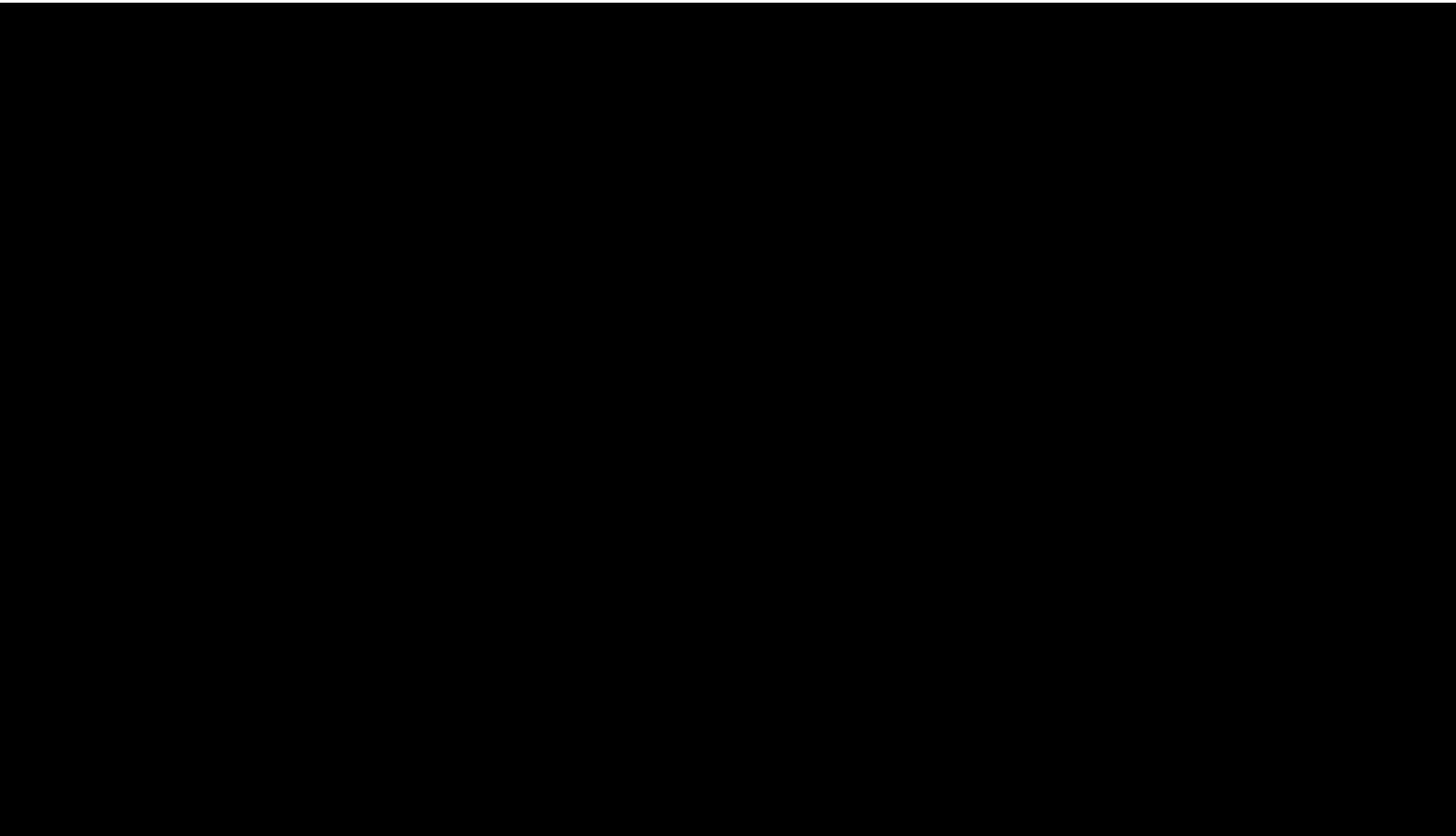
DOCTOR OF PHILOSOPHY

in

Developmental and Stem Cell Biology

in the

GRADUATE DIVISION

of the

UNIVERSITY OF CALIFORNIA, SAN FRANCISCO

For Dominique,

Without whom this wouldn't have been possible

Acknowledgements

Surviving graduate school would not have been possible without the intellectual and emotional support of a small army of individuals. To them I am forever grateful. However, several people need to be mentioned specifically. Thank you David for the opportunity. Thank you Shawn for always being there when I needed you. Without you, this project would have been stuck in its infancy indefinitely. You perfectly modeled how I want to be scientifically as I mature in this chosen career path. Thank you Jake for being the best friend I never knew I needed. Your friendship was one of the strongest emotional rocks I leaned upon when times were hard. Finally, thank you Dominique for being the foundation from which I was able to ground myself for years on end. Without your continuous support, I believe I would have given up at various times. Your belief in me carried me forward when my belief in myself could not. I will always love you for that.

Abstract

Prominent Postnatal Streams Of Interneurons In The Ferret Cortex

By

Justin K. Ellis, MD

Recent work shows that human brain development continues extensively into the postnatal period as specific cortical circuits continue to receive streams of late migrating interneurons. Rodent models of this phenomenon either fail to identify similar contributions or reveal much smaller migrating populations of cells. I asked whether the ferret, a gyrencephalic mammal with large increases in brain size after birth, possesses postnatal streams of young interneurons like in the human. I sectioned the brains of ferret kits at P20 (equivalent to human term), P40, P65 and P90 and stained for Doublecortin (DCX), a marker expressed by young neurons. In addition to the rostral migratory stream to the olfactory bulb, three additional streams were discovered in the white matter at P20: one oriented rostrally towards the prefrontal cortex, one oriented dorsally towards the posterior sigmoid gyrus, and one oriented caudally towards the occipital cortex. Each stream diminished at a unique rate before disappearing by P90. The DCX+ cells in each stream expressed GAD67, as well as a molecular signature consistent with cells born in the caudal ganglionic eminence. Young interneurons were observed transitioning from the white matter to the cortex over time, and only small percentages appeared to undergo apoptosis or remain in the white matter until adulthood. My work shows that the ferret brain possesses robust postnatal streams of

young interneurons oriented towards cortical destinations, perhaps suggesting that this

phenomenon is a common method used to build large gyrencephalic brains.

Table of Contents

List of Figures

Chapter 5. Majority of DCX+ interneurons appear to be transitioning into the cortex

List of Abbreviations

Symbol	Definition
ASG	Anterior Sigmoid Gyrus
BG	Basal Ganglia
CG	Coronal Gyrus
DCX	Doublecortin
DG	Dentate Gyrus
DMS	Dorsal Migratory Stream
GAD67	Glutamic Acid Decarboxylase 67
GFAP	Glial Fibrillary Acidic Protein
LV	Lateral Ventricle
MBP	Myelin Basic Protein
MMS	Medial Migratory Stream
OB	Olfactory Bulb
OCTX	Occipital Cortex
OG	Orbital Gyrus
PMS	Posterior Migratory Stream
PSG	Posterior Sigmoid Gyrus
PV	Parvalbumin
RMS	Rostral Migratory Stream
SCGN	Secretogoggin
SST	Somatostatin

THL   Thalamus

Chapter 1

Introduction

In human brain development, the early postnatal period is characterized by rapid growth and adaptation to the ex utero world. It is also a period of marked vulnerability to environmental insults, such as hypoxia, that can result in cognitive deficits later in life, as well as an increased risk for psychiatric disease. Despite its importance to development and relevance to disease, relatively little is known about postnatal development of cortical circuits.

Human Postnatal Interneuron Migration

Recent work in human post-mortem tissue has revealed multiple streams of late migrating interneurons oriented towards specific cortical regions throughout the first eighteen months of life (**Fig 1.1**). In fact, humans possess at least three postnatal streams of migrating interneurons; a rostral migratory stream (RMS) that supplies multiple subtypes of interneurons to the olfactory bulbs and disappears by 12 months, a medial migratory stream (MMS) that branches off of the RMS, putatively supplies Calretinin+ interneurons to the ventromedial
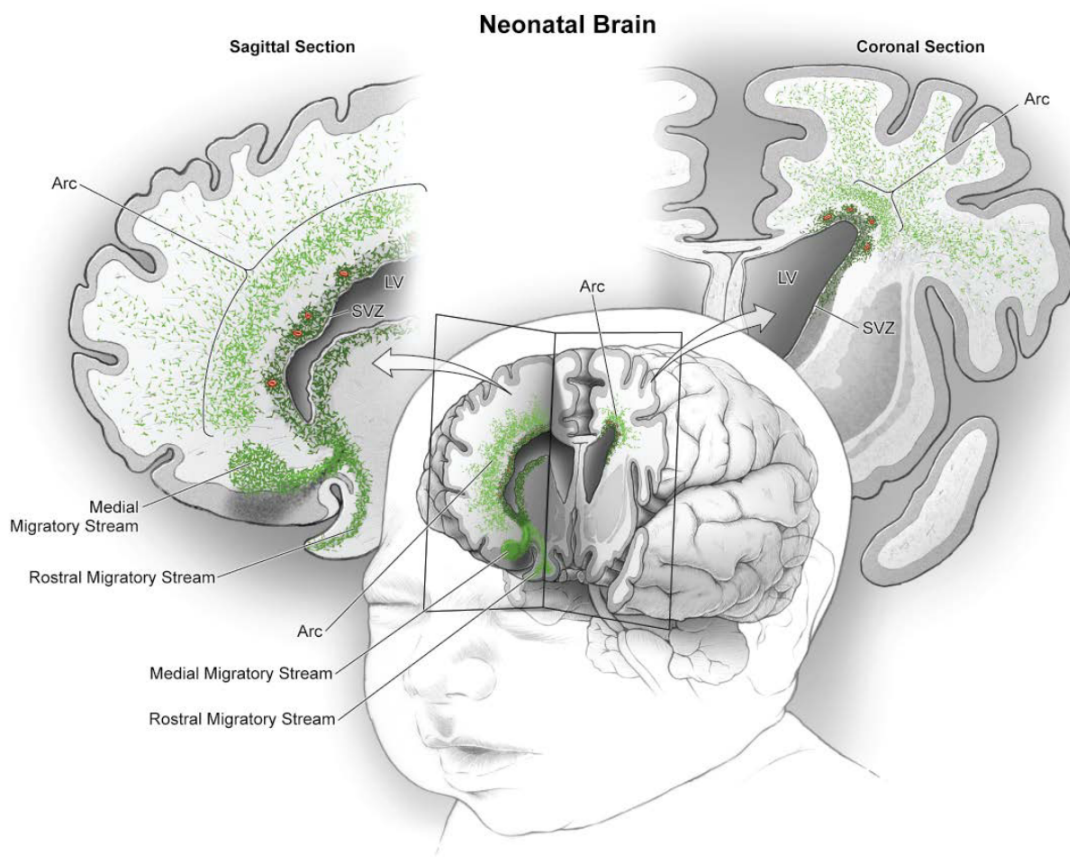
Paredes et al, Science, 2016

Figure 1.1 Postnatal migrating interneurons in human brain

prefrontal cortex (VMPFC) and disappears by 12 months (Sanai 2011), and a dorsal migratory arc of cells that is present at the rostral tip of the lateral ventricle and putatively supplies multiple subtypes of interneurons to the anterior cingulate cortex (ACC) and superior frontal gyrus (SFG) and disappears by 5 months (Paredes 2016).

However, in humans, the study of postnatal migrating interneurons and their contributions to cortical development is confounded by the restrictions inherent in using post-mortem tissue, and many vital questions remain. Fate mapping studies cannot be performed, nor can cause and effect relationships be elucidated. Most importantly, it is unknown to which cortical circuits these neurons contribute and how vulnerable they are to injury. What is needed is an appropriate animal model.

Rodent Postnatal Interneuron Migration

Postnatal migration of interneurons has begun to be characterized in mice, and it was discovered that they possess a population of postnatal migrating 5HT3a+ cells that exit the RMS up to postnatal day 10 and terminate in layer six of the orbitofrontal cortex (Inta 2008). However, the number of postnatal migrating cells is small and does not reflect the subtype diversity seen in human. Furthermore, there is no evidence that mice possess a dorsal migratory stream, like in human. Finally, the mouse equivalency of human term is considered to be postnatal day 10, which is when these cells are seen to cease migrating into the cortex. Therefore, it is unclear if what is observed in rodents constitutes true postnatal migration in comparison with human as the phenomenon does not continue past the equivalency of human term. Although rats have larger brains than mice, they have not been evaluated in terms of postnatal migration of interneurons.

Recent evidence suggests that larger mammalian species, such as pigs, may more closely resemble humans in terms of postnatal migration of interneurons (Morton 2017). However, the cost and care of pigs is quite large, and many of the same difficulties arise as when working with human postmortem tissue; creating transgenic animals would be extremely difficult and little to no *in vivo* manipulation of circuitry has ever been performed.

Ferret Postnatal Brain Development

Ferrets have been used as an animal model to study brain development for many years and are considered an attractive model for many reasons. Ferrets, unlike rodents, have a significantly increased brain size, a gyrencephalic cortex, extended postnatal development, and a variety of other features that make them more similar to primate brain development than rodents (McConnell 1985, McConnell 1988). Because of these reasons, I hypothesized that ferrets would reflect the postnatal migration of interneurons seen in humans more closely than that seen in rodents.

Chapter 2

Materials and Methods

Section 1: Animals and tissue processing

<u>Animals</u>

Pregnant jills were obtained from Marshall Farms (North Rose, NY) at E26 gestation. All animal experiments were conducted in strict accordance with institutional guidelines and the Guide for the Care and Use of Laboratory Animals, published by the National Institutes of Health. All experiments were approved by the Institutional Animal Care and Use Committee at UCSF.

<u>Tissue processing</u>

Ferret kits were deeply anesthetized using an isoflurane vaporizer and transcardially perfused with 0.1M phosphate-buffered saline (PBS) at pH 7.4 followed by 4% paraformaldehyde (PFA) in PBS at pH 7.4. Brains were dissected from the skull and fixed in 4% PFA overnight at 4^0C. After fixation, brains were cryoprotected in 30% sucrose in 0.1M PBS until the brains sunk. For sectioning, brains were frozen to the stage of a sliding microtome (Leica SM2010R). Coronal, sagittal and horizontal floating sections (50um) were cut. Cut sections were stored in 6 well cell culture plates in 0.1M PBS with azide at 4^0C and were used for free floating immunohistochemistry.

Section 2: Antibody characterization

The rabbit polyclonal anti-doublecortin antibody (Cell Signaling Technology) was characterized by the manufacturer in a Western blot analysis of fetal rat brain tissue lysate, yielding a single protein band at ~45kDa. We confirmed this in ferret by performing a Western blot analysis of postnatal day 20 whole brain lysate and observing a similar band. Furthermore, in the current study this antibody specifically stained the cytoplasm of cells with a classic migratory morphology as would be expected.

The guinea pig polyclonal anti-doublecortin antibody (Millipore Bioscience Research) was characterized by the manufacturer in a Western blot analysis of rat brain tissue lysate, yielding a single protein band at ~45KDa. We confirmed this in ferret by performing a Western blot analysis of postnatal day 20 whole brain lysate and observing a similar band. Furthermore, in the current study this antibody specifically stained the cytoplasm of cells with a classic migratory morphology as would be expected.

The goat polyclonal anti-GAD67 antibody (Abcam) was characterized by the manufacturer in Western blot analyses of both mouse and human brain lysate, yielding a single protein band of 70KDa. We confirmed this in ferret by performing a Western blot analysis of postnatal day 20 whole brain lysate and observing a similar band.

The mouse monoclonal anti-GFAP antibody (Sigma Aldrich) was characterized by the manufacturer by performing a Western blot analysis of whole extract of rat B35 cells, yielding a band of ~50KDa. We confirmed this in ferret by performing a Western blot analysis of postnatal day 20 whole brain lysate and observing a similar band.

The mouse monoclonal anti-Olig2 antibody (gift from Chuck Stiles lab) was previously characterized by Lu et al, Neuron, 2000 and identifies oligodendrocytes. We further characterized this antibody in ferret by performing a Western blot analysis of

postnatal day 20 whole brain lysate and observing a band at 57KDa, as would be expected.

The goat polyclonal anti-Sox10 antibody (Santa Cruz Biotechnology) was characterized by the manufacturer by performing a Western blot analysis on both non-transfected and mouse and human recombinant transfected 293T whole cell lysates, yielding a single protein band at 55KDa. We characterized this antibody in ferret by performing a Western blot analysis of postnatal day 20 whole brain lysate and observing a similar band.

The rabbit polyclonal anti-Iba1 antibody (Wako Chemcials) was characterized by the manufacturer by performing a Western blot on isolated rat microglia, yielding an appropriate band at 17KDa.

The mouse monoclonal anti-Coup-TFII antibody (Perseus Proteomics) was characterized by performing a Western blot analysis on ferret postnatal day 20 whole brain lysate and observing a single protein band at 45KDa. Furthermore, in the current study, immunohistochemistry of P1 ferret tissue revealed positive staining of the caudal ganglionic eminence, and not the medial ganglionic eminence, as would be expected.

The rabbit polyclonal anti-Nkx2.1 antibody (Santa Cruz Biotechnology) was characterized by the manufacturer by performing a Western blot analysis on human Nkx2.1 transfected 293T whole cell lysate and revealing a single band between 38-42KDa. We characterized this antibody by performing a Western blot analysis on ferret postnatal day 20 whole brain lysate and observing a similar band.

The goat polyclonal anti-Sp8 antibody (Santa Cruz Biotechnology) was characterized by Radonjic et al, Front Neuroanat, 2014 who performed a Western blot

on human fetal cerebral cortex, yielding a band at ~50KDa. We characterized this antibody by performing a Western blot on postnatal day 20 ferret whole brain lysate and observing a similar band.

The rabbit polyclonal anti-Secretogogin antibody (Sigma Aldrich) was characterized by Sanaganarapu et al, PLOS ONE, 2016 by performing a Western blot on BRIN-BD11 insulinoma cell lysates, yielding a single protein band of ~32KDa. We characterized this antibody by performing a Western blot analysis on postnatal day 20 ferret whole brain lysate and observing a similar band.

The goat polyclonal anti-Somatostatin antibody (Santa Cruz Biotechnology) was characterized by the manufacturer by performing a Western blot analysis on non-transfected and transfected 293 whole cell lysates, yielding a single protein band of 13-15KDa. We characterized this antibody by performing a Western blot analysis on postnatal day 20 ferret whole brain lysate and observing a similar band.

The rabbit polyclonal anti-Parvalbumin antibody (Swant) was characterized by the manufacturer by performing immunohistochemical stains on wild type and parvalbumin knockout mice.

The mouse monoclonal anti-Calretinin antibody (Swant) was characterized by the manufacturer by performing immunohistochemical stains on wild type and calretinin knock out mice.

The rabbit monoclonal anti-Cleaved Caspase 3 antibody (Cell Signaling) was characterized by the manufacturer by performing Western blot analyses on control and cytochrome c-treated HeLa, NIH/3T3, and C6 cells and observing two protein bands at 17 and 19KDa.

The rat monoclonal anti-myelin basic protein antibody (Abcam) was characterized by the manufacturer by performing a Western blot analysis on mouse brain lysate, yielding two isoforms at 19 and 26KDa.

Section 3: Immunohistochemistry, confocal and epifluorescent microscopy, and image processing

<u>Staining</u>

All doublecortin and GAD67 immunohistochemistry was performed using tyramide signal amplification. In short, free floating sections (50um) were first mounted on glass slides and allowed to dry for one hour. Slides were then rinsed in PBS, and antigen retrieval was performed at 95^0C in 0.01M Na Citrate buffer, pH=6. Durations of antigen retrieval can be found in Table 1. Following antigen retrieval, slides were washed with PBS-T (0.2% TX100 in PBS) for 15 minutes, incubated with 0.02N HCl in PBS for 30 minutes at room temperature (RT), and then blocked with TNB solution (0.1 M Tris-HCl, pH 7.5, 0.15 M NaCl, 0.5% blocking reagent from PerkinElmer) for 1 hour at RT. Slides were incubated in primary antibodies overnight at 4°C (see table 1). All antibodies were diluted in TNB solution. The following day, slides were rinsed in PBS-T for 1 hour at RT and then incubated with biotinylated secondary antibodies at (1:500) (Jackson Immunoresearch Laboratories), as well as any Alexa secondaries being used at (1:750), for 1 hour at room temperature. Sections were then incubated for 30 min in streptavidin-horseradish peroxidase that was diluted (1:200) with TNB. Finally, sections were incubated in tyramide-conjugated fluoroscein for 5 minutes at 1:100. Slides were

then covered with glass cover slips using DAPI Fluoromount-G (Thermo Fisher Scientific).

Primary antibodies not receiving tyramine signal amplification were stained in the following manner. Free floating sections (50um) were first mounted on glass slides and allowed to dry for one hour. Slides were then rinsed in PBS, and antigen retrieval was performed at 95^0C in 0.01M Na Citrate buffer, pH=6. Durations of antigen retrieval can be found in Table 1. Following antigen retrieval, slides were washed with PBS-T (0.2% TX100 in PBS) for 15 minutes, blocked for one hour in blocking solution (10% goat or donkey serum in 0.1M PBS w/ 0.2% Triton-X) and incubated with primary antibody in blocking solution overnight at 4^0C. Sections were washed 6 times for 10min each in PBS-T on a rocker at room temperature. Sections were then incubated for two hours with Alexa secondary antibody in blocking solution (1:750). Sections were then washed 6 times for 10min each in washing solution. Sections were covered with cover slips using DAPI Fluoromount-G.

Confocal and epifluorescent microscopy

All confocal images were taken using a Leica Sp8 confocal microscope (Leica Microsystems, Wetzlar, Germany). Images were acquired as 2um thick optical sections. Tile scans used for mapping doublecortin signal were taken using a Zeiss Axioimager (Carl Zeiss, Oberkochen, Germany).

Image processing

Lif files were covered to tif files using ImageJ. All image files were imported into Photoshop CS6 and adjusted for brightness and contrast.

Section 4: Map Making

Tile scans of DCX stained P20 ferret brain sections in the sagittal, coronal, and horizontal planes were uploaded into Adobe Illustrator CS6. The outline of each section was traced using the pen tool. DCX+ cell bodies exhibiting an elongated morphology characteristic of a migrating cell were identified and marked with an individual dot.

Section 5: Cell counting and quantification

DCX+ Bulge quantifications

DCX+ bulges for each of the three streams were compared at P20, P40, P65, and P90. Confocal images of each bulge were uploaded into ImageJ. The anterior and posterior borders of each bulge were visually determined, and a line was drawn representing the maximum possible length of each bulge. Three sections from each of three animals were included for each stream and each time point. Distances in microns were recorded, and Student's t tests were performed on the average distance taken for each animal using Prism version 6, Graphpad. Significance was set at $p=0.05$.

DCX+ cell densities

Confocal images were obtained for each stream proximal to the DCX+ bulge. Images were taken at P20, P40, P65, and P90. Three sections from each of three animals were included for each stream and each time point. Images were loaded into ImageJ, and DCX+ cell bodies were counted. The DCX+ cell density was calculated by dividing the number of cells per section by the area of the section multiplied by the tissue thickness (50um). Student's t-tests were performed on the average number of cells per animal using Prism version 6, Graphpad. Significance was set at $p=0.05$.

<u>DCX co-localizations</u>

Confocal images were taken of the medial migratory stream in the sagittal plane at the indicated ages and were loaded into ImageJ. Percent co-localizations were calculated by counting the number of DCX+ cell bodies per image and dividing by the number of co-localized cells. Three sections from each of three animals were counted.

<u>White matter cells and caspase+ cells</u>

Sagittal sections of the medial migratory stream were stained with either secretogogin or cleaved caspase 3 at the indicated ages and were visually inspected using a confocal microscope. SCGN+ cells in the white matter with a mature, differentiated morphology were counted live. All SCGN+ cells in the MMS were included in each count. Cleaved caspase 3+ cells in the white matter were counted live. All positive cells in the MMS were included in each count. Three sections from each of three animals were counted. Student's t-tests were performed to determine significance using Prism version 6, Graphpad.

Section 6: iDISCO+

<u>Clearing and staining</u>

iDISCO+ protocol is from Renier et al, Cell, 2016. In brief, ferrets were transcardially perfused at P20 and postfixed O/N. Brains were extracted and cut in half. Individual hemispheres were stored in PBS azide until ready to be utilized. Fixed samples were washed in PBS for 1h twice, then in 20% methanol (in ddH2O) for 1h, 40% methanol for 1h, 60% methanol for 1h, 80% methanol for 1h, and 100% methanol for 1h twice. Samples were then bleached with 5% H2O2 (1 volume of 30%

H2O2 for 5 volumes of methanol, ice cold) at 4°C overnight. After bleaching, samples were re-equilibrated at room temperature slowly and re-hydrated in 80% methanol in H2O for 1h, 60% methanol / H2O for 1h, 40% methanol / H2O for 1h, 20% methanol / H2O for 1h, and finally in PBS / 0.2% TritonX-100 for 1h twice. Pre-treated samples were then incubated in PBS / 0.2% TritonX-100 / 20% DMSO / 0.3M glycine at 37°C for 36h, then blocked in PBS / 0.2% TritonX-100 / 10% DMSO / 6% Donkey Serum at 37°C for 2 days. Hemispheres were then incubated in primary antibody dilutions of 1:100 in PBS-Tween 0.2% with Heparin 10µg/mL (PTwH) / 5% DMSO / 3% Donkey Serum at 37°C for 7 days. Primary antibody solutions were changed ever other day. Samples were then washed in PTwH for 24h (5 changes of the PTwH solution over that time), then incubated in secondary antibody dilutions (e.g. donkey anti-rabbit-Alexa647 at 1:500 in PTwH / 3% Donkey Serum) at 37°C for 4 days. Samples were finally washed in PTwH for 1d before clearing and imaging.

Immunolabeled brains were cleared with the following method. Samples were dehydrated in 20% methanol (in ddH2O) for 1h, 40% methanol / H2O for 1h, 60% methanol / H2O for 1h, 80% methanol / H2O for 1h, and 100% methanol for 1h twice. Samples were incubated overnight in 1 volume of Methanol / 2 Volumes of Dichloromethane (DCM, Sigma 270997-12X100ML) until they sank to the bottom of the vial (50ml falcon tubes were used throughout the process). The sample was then washed for 20min twice in 100% DCM. Finally, samples were incubated (without shaking) in DiBenzyl Ether (DBE, Sigma 108014-1KG) until clear (about 30min) and stored in DBE at room temperature.

Light sheet and spinning disk microscopy

Cleared samples were imaged on a light-sheet microscope (Custom built AZ-100 by Nikon Imaging Center, UCSF) equipped with a sCMOS camera (Andor Neo) and a 2X (WD=45mm, N.A.=0.2) or 5X (WD=15mm, N.A.=0.5) objective lens. Scans were made at either a 1X or 2X zoom magnification. The samples were scanned with a step-size of 16µm (2X Obj.) or 2.3um (5X obj.).

Higher magnification images were taken of each sample using the 10X objective on a spinning disk microscope (Yokagawa CSU22).

Image processing

All image and movie files were processed and snapshots taken using Imaris v. 7.22. Brightness and contrast were the only attributes adjusted.

Chapter 3

Ferrets possess prominent postnatal streams of DCX+ cells

To investigate the existence of postnatal migrating interneurons in the ferret brain, I began by staining P20 sagittal, coronal, and horizontal tissue sections with doublecortin (DCX). P20 was chosen as a starting point, as it is thought to be equivalent to human term in regards to percent maximum brain growth (**Fig. 3.1**). Furthermore, at P20, the ferret brain has transitioned from a developing lissencephalic cortex to a six layered gyrencephalic cortex.

At P20, DCX+ cells were widely distributed throughout the cortex and white matter. However, DCX+ cells in the cortex had a strikingly different morphology than those in the white matter (**Fig. 3.2**). In the cortex, DCX+ cells possessed large, round cell bodies and multiple processes. In contrast, in the white matter, DCX+ cells mostly possessed a classic migratory morphology, i.e. an elongated cell body along with a single leading process (**Fig. 3.2**). The leading process was sometimes seen to be forked, as would be expected for a migrating cell.

Focusing exclusively on the DCX+ cells in the white matter with a migratory morphology, I surveyed the P20 ferret brain in all three orientations by taking 5 sections of tissue, 1mm apart, for each orientation. Sections were then stained with DCX, tiled using an epifluorescent microscope (Nikon), and loaded into Adobe Illustrator. Next, I made maps of each DCX+ cell body with a migratory morphology by placing a mark on
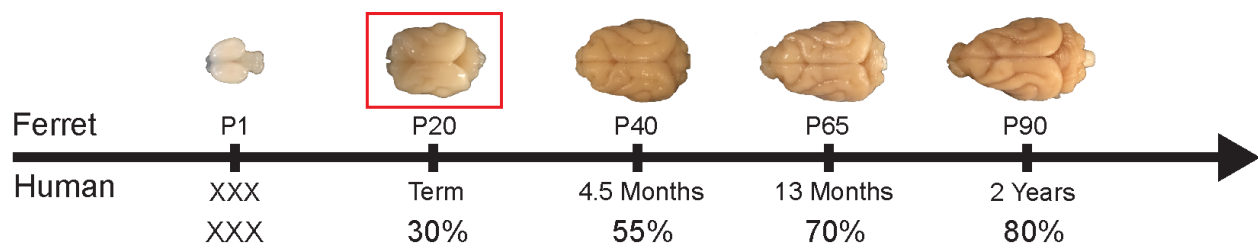
Ferret	P1	P20	P40	P65	P90
Human	XXX	Term	4.5 Months	13 Months	2 Years
	XXX	30%	55%	70%	80%

Figure 3.1. Comparison of ferret and human developmental timeline

By using percent maximum brain weight, ferret brain development can be aligned with human to determine at what age ferret brain is equivalent to human term. At P20, both ferret and human brain are 30% of their maximum brain weight.
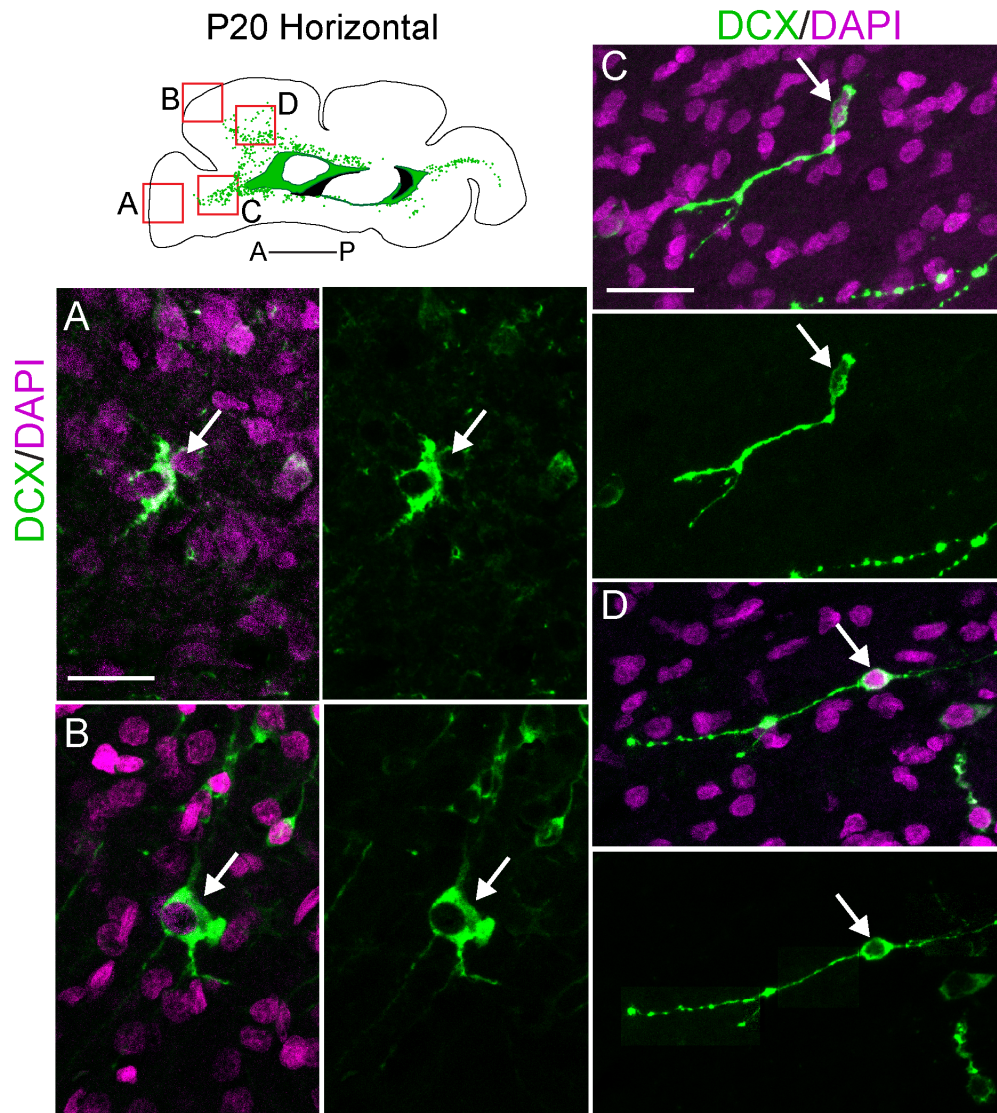
P20 Horizontal

DCX/DAPI

Figure 3.2. DCX+ cells in the P20 ferret cortex and white matter exhibit different morphologies.

A,B: DCX+ cells in the cortex have large, rounded cell bodies and multiple extended processes. **C,D:** DCX+ cells in the white matter exhibit a migratory morphology including an elongated cell body and a single, sometimes forked, leading process. Scale bar = 10um.

top of each cell (**Fig. 3.3**). The maps revealed a highly prominent population of DCX+ cells distributed throughout the P20 ferret brain. In the sagittal orientation, a larger proportion of cells appeared to be concentrated in the most medial sections compared to lateral. In the coronal orientation, a larger proportion of cells appeared to be concentrated in the most rostral sections compared to caudal. In the horizontal orientation, a larger proportion of cells appeared to be concentrated in the dorsal and middle sections compared to the more ventral sections.

Closer inspection of these maps revealed that multiple populations of DCX+ cells appeared organized throughout the brain in streams of cells oriented away from the lateral ventricles and towards different regions of cortex. In fact, three such streams could be appreciated. In the sagittal orientation, it was quite apparent that a prominent collection of cells appeared to be branching off the rostral migratory stream and oriented towards the prefrontal cortex, i.e. the orbital gyrus and anterior sigmoid gyrus (**Fig. 3.4**). I refer to this stream as the medial migratory stream as multiple characteristics mimic the MMS that has been characterized in human. For instance, DCX+ cells appeared to exit the RMS in chains before dispersing into a individual cells farther away. In the horizontal orientation, the MMS could be appreciated exiting a large bulge of DCX+ cells.

I next wanted to evaluate how this stream changed over time, so I stained tissue in the sagittal and horizontal planes at P40, P65, and P90 (**Fig 3.5**). In the sagittal orientation, both the chains and the proportion of individual cells decreased significantly between P20 and P40, as well as between P40 and P65. By P90, the stream had disappeared entirely. In the horizontal plane, the DCX+ bulge and the stream of
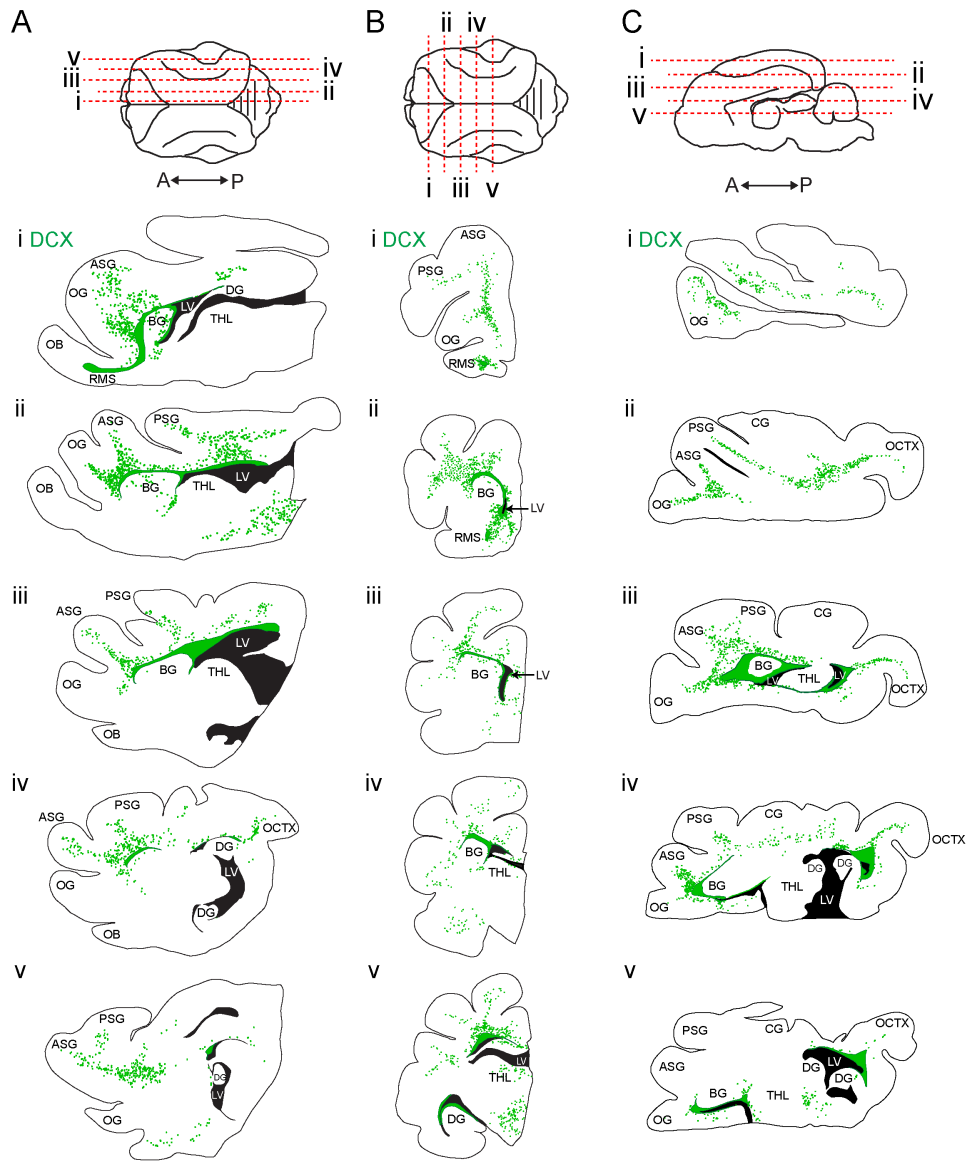
Figure 3.3. Ferret P20 possesses robust populations of DCX+ cells with a migratory morphology.

In P20 ferret there are significant numbers of DCX+ cells with a migratory morphology visible in sagittal **(A)**, coronal **(B)**, and horizontal orientations **(C)**.
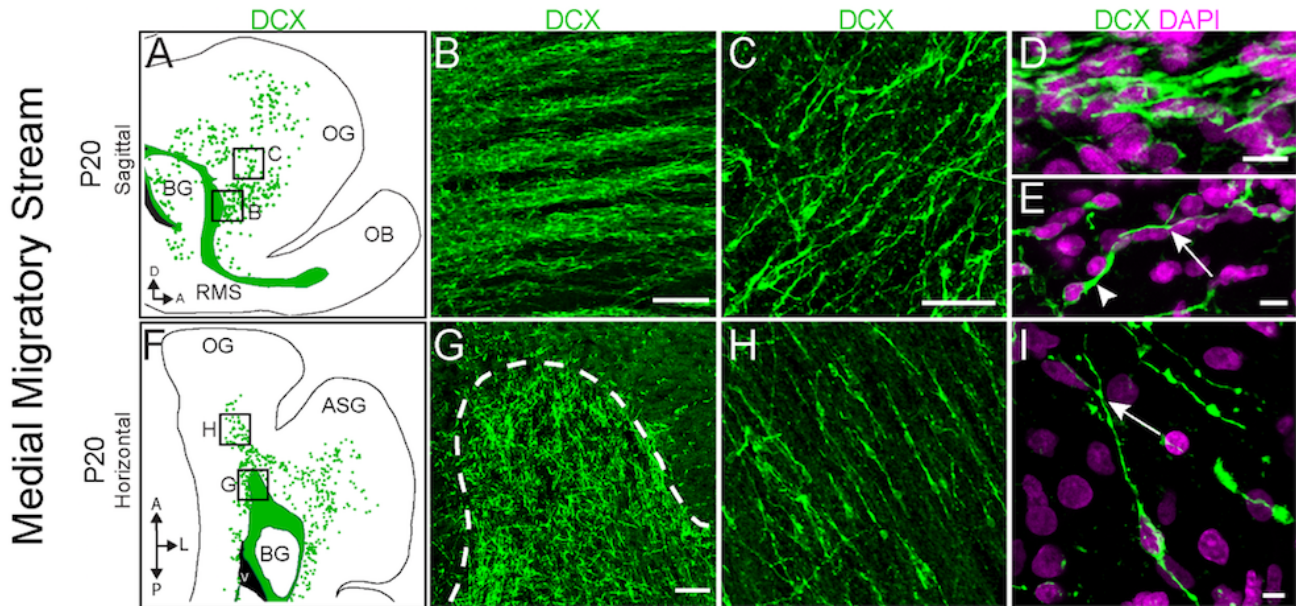
Figure 3.4. Ferrets possess a medial migratory stream at P20

A: Sagittal map highlighting MMS exiting the RMS and oriented towards the PFC, i.e. the OG and ASG. **B,D:** DCX+ chains exiting the RMS, high mag pic of DCX+ chain.

C,E: Highly dense population of DCX+ cells, high mag pic of DCX+ cell with an elongated cell body and forked leading process. **F:** Horizontal map highlighting the MMS. **G:** DCX+ bulge anterior to the BG. **H:** DCX+ cells oriented away from the bulge and towards the PFC. **I:** Example of individual DCX+ cell with migratory morphology. Scale bar = 25um and 10um.
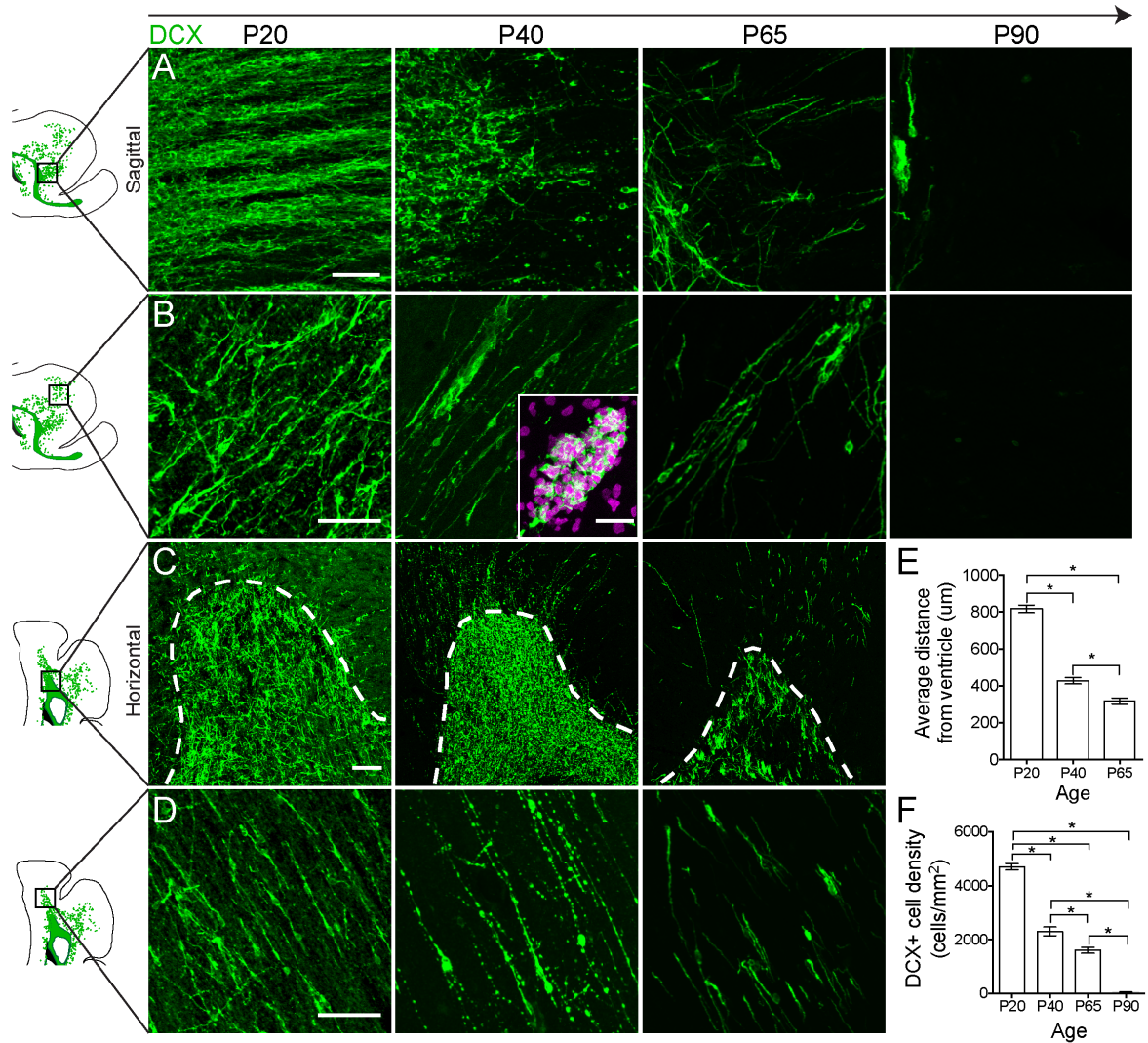
Figure 3.5. Ferret MMS disappears by P90.

A,B: In the sagittal plane, both the chains exiting the RMS and the individual cells decrease over time and have disappeared completely by P90. **C,D:** In the horizontal plane, both the DCX+ bulge, and the individual cells decrease over time and have completely disappeared by P90. **E:** Quantification of the decrease in DCX+ bulge size over time. **F:** Quantification of the decrease in DCX+ cell density over time. Scale bar = 25um.

individual cells decreased significantly over time, and that significant decrease is quantified.

Between P20 and P40, it was observed that the widely distributed, individual DCX+ cells in the MMS condensed into large clusters of cells. This was most appreciated in the coronal plane (**Fig. 3.6**). These clusters decreased in number by P65 and had disappeared completely, as with the stream, by P90.

The sagittal plane also revealed a dorsal stream of DCX+ cells oriented away from the lateral ventricle and towards the posterior sigmoid gyrus. I refer to this stream as the Dorsal Migratory Stream (**Fig. 3.7**). Just dorsal to the lateral ventricle is a large bulge of DCX+ cells that disperses into a stream of cells. In order to evaluate how this stream changed over time, I stained tissue in the sagittal and coronal planes at P40, P65, and P90 (**Fig. 3.8**). By P40, the bulge had decreased significantly, and the stream had almost completely disappeared. By P65, the bulge had decreased in size significantly again, and the stream had finished. Both of these results were quantified.

The sagittal plane revealed one final stream, one that I refer to as the Posterior Migratory Stream. This stream appears oriented away from the lateral ventricles and towards the occipital cortex (**Fig. 3.9**). Once again, cells appear to be exiting a large DCX+ bulge located adjacent to the ventricle before dispersing into a stream. Both the bulge and the stream decrease significantly by P40 before disappearing altogether by P65 (**Fig. 3.10**).
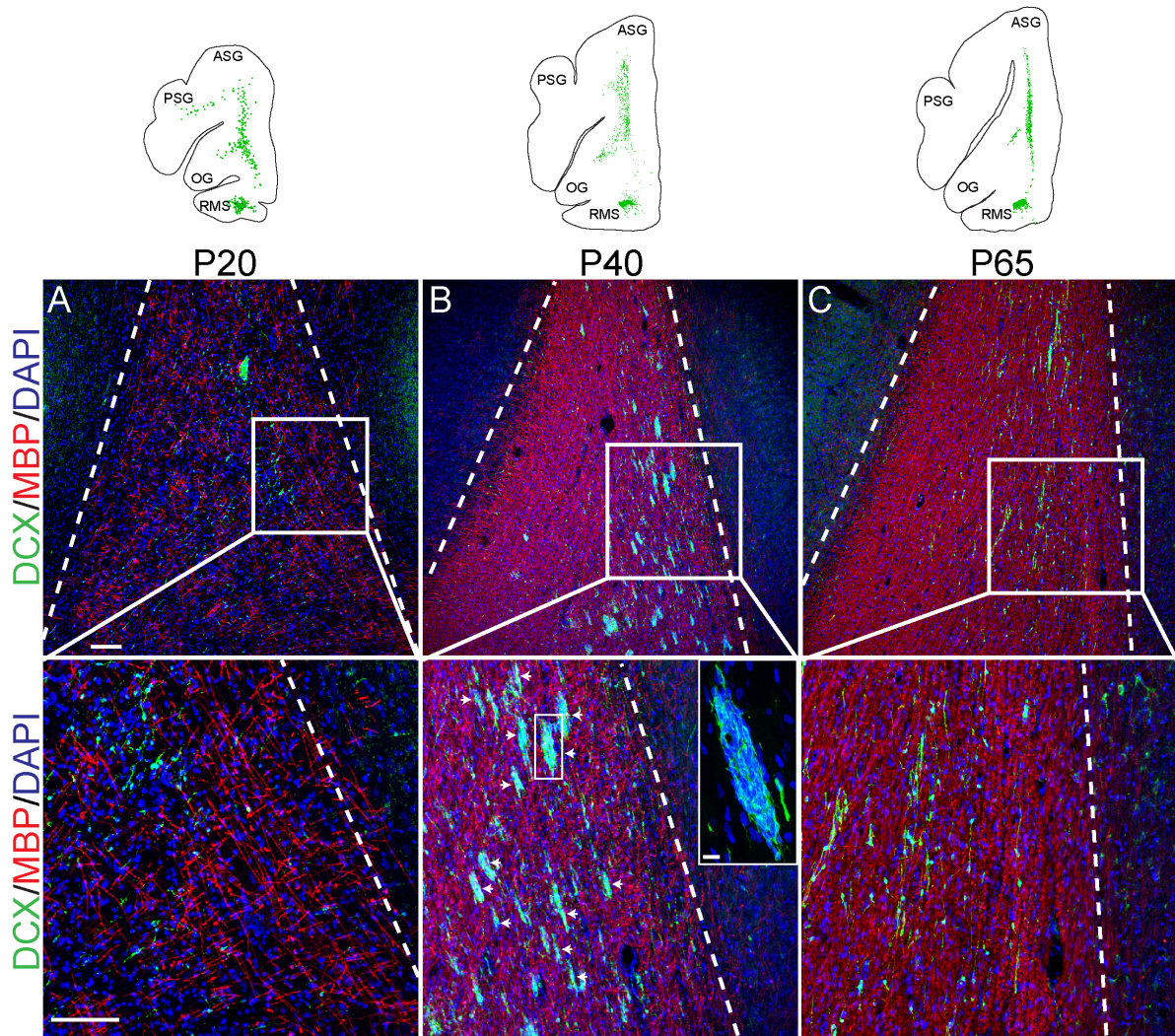
Figure 3.6. DCX+ cells in the MMS condense into clusters by P40

A: Coronal orientation, DCX+ cells at P20 are seen individually oriented throughout the white matter tract. **B:** By P40, individual cells have condensed into clusters. **C:** By P65, both the clusters and individual cells have decreased in number. Scale bar = 25um.
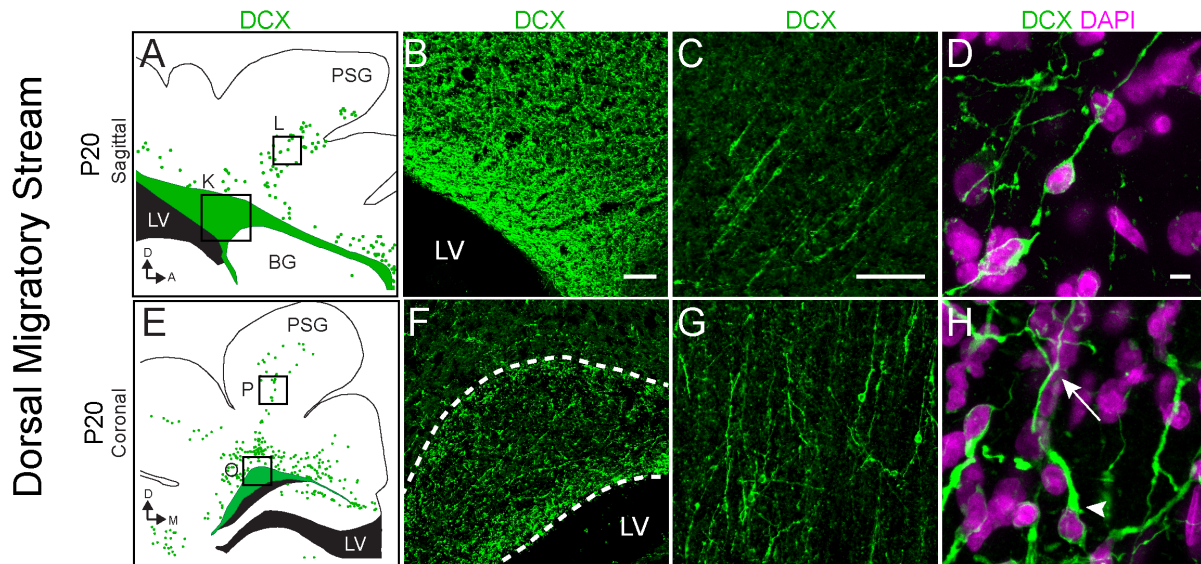
Figure 3.7. Ferrets possess a dorsal migratory stream at P20

A: Sagittal map highlighting the DMS exiting the DCX+ bulge adjacent to the lateral ventricle and oriented towards the PSG. **B:** DCX+ bulge. **C,D:** Highly dense population of DCX+ cells, high mag pic of DCX+ cell with an elongated cell body and forked leading process. **E:** Coronal map highlighting the DMS. **F:** DCX+ bulge. **G:** DCX+ cells oriented away from the bulge and towards the PSG. **H:** Example of individual DCX+ cell with migratory morphology. Scale bar = 25um and 10um.
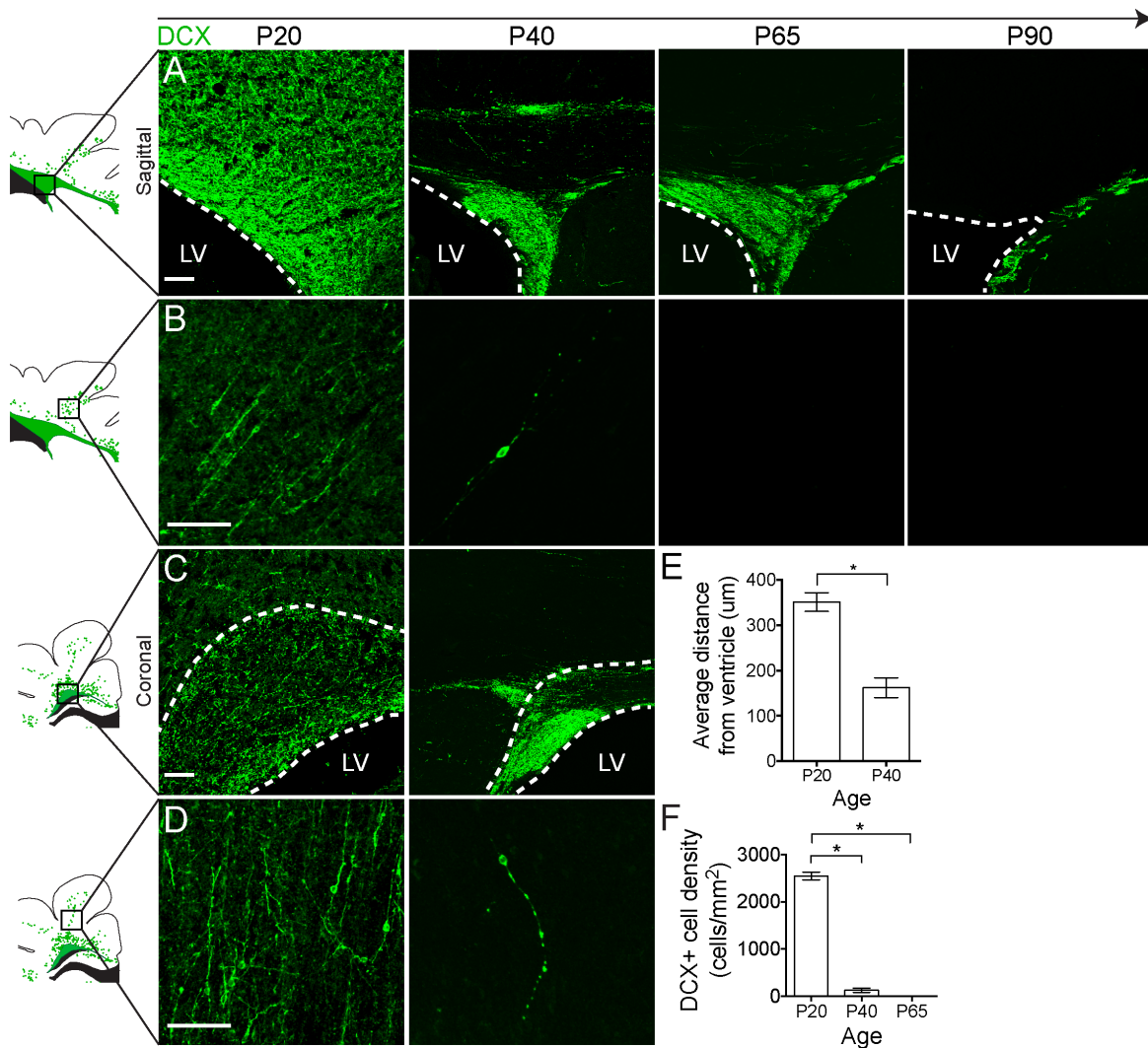
Figure 3.8. Ferret DMS disappears by P40

A,B: In the sagittal plane, both the DCX+ bulge and the individual cells decrease over time and have disappeared by P40. **C,D:** In the coronal plane, both the DCX+ bulge and the individual cells decrease over time and have disappeared by P40. **E:** Quantification of the decrease in DCX+ bulge size over time. **F:** Quantification of the decrease in DCX + cell density over time. Scale bar = 25um.
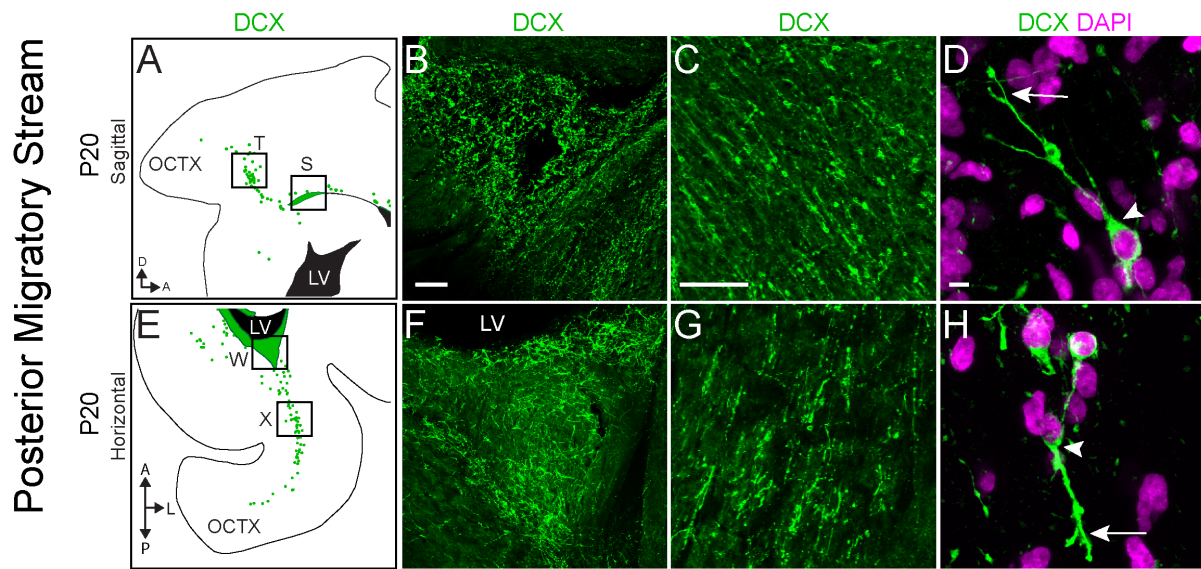
Figure 3.9. Ferrets possess a posterior migratory stream at P20

A: Sagittal map highlighting PMS oriented towards the OCTX. **B:** DCX+ bulge adjacent to the lateral ventricle. **C,D:** Highly dense population of DCX+ cells, high mag pic of DCX+ cell with an elongated cell body and forked leading process. **E:** Horizontal map highlighting the PMS. **F:** DCX+ bulge. **G:** DCX+ cells oriented away from the bulge and towards the OCTX. **H:** Example of individual DCX+ cell with migratory morphology. Scale bar = 25um and 10um.
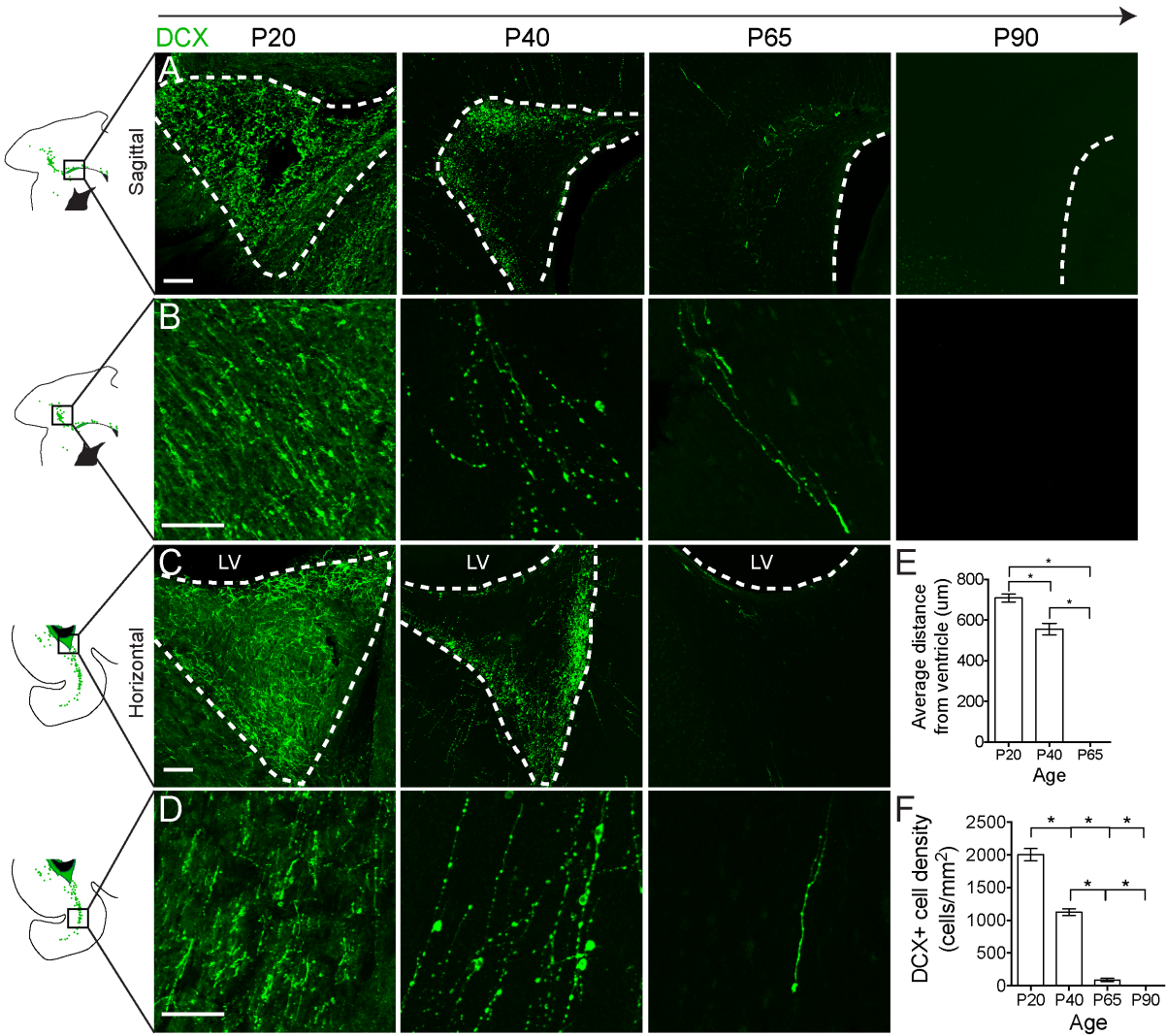
Figure 3.10. Ferret PMS disappears by P65

A,B: In the sagittal plane, both the DCX+ bulge and the individual cells decrease over time and have disappeared completely by P65. **C,D:** In the horizontal plane, both the DCX+ bulge, and the individual cells decrease over time and have completely disappeared by P65. **E:** Quantification of the decrease in DCX+ bulge size over time. **F:** Quantification of the decrease in DCX+ cell density over time. Scale bar = 25um.

Chapter 4

Doublecortin+ cells express markers of caudal ganglionic eminence derived interneurons

Having identified three streams of DCX+ cells with a migratory morphology in the white matter of the postnatal ferret brain, I next wanted to know if these DCX+ cells expressed markers of interneurons. Sagittal slices of P20 ferret tissue were stained with a variety of antibodies for neuronal markers. 100% of DCX+ cells co-expressed GAD67 (**Fig. 4.1**), a definitive marker of interneurons. This percent co-localization did not change between P20 and P40. DCX+ cells did not express NeuN (data not shown), a marker of mature neurons. Furthermore, DCX+ cells did not express markers of glial cells, such as GFAP, a marker of astrocytes, OLIG2 and SOX10, markers of oligodendrocytes, or Iba1, a marker of microglial cells (**Fig. 4.2**). This data set was repeated in the caudal region of the brain (dotted line), and the results were the same. From these data, I concluded that Dcx+ cells with a migratory morphology were young interneurons.

To further characterize the interneuronal origin of DCX+ cells, I first stained P1 coronal and sagittal sections for the proteins, COUP-TFII and Nkx2.1, markers of the caudal ganglionic eminence and medial ganglionic eminence, respectively (**Fig. 4.3**). Each antibody appropriately identified the CGE and MGE in the newborn ferret brain.
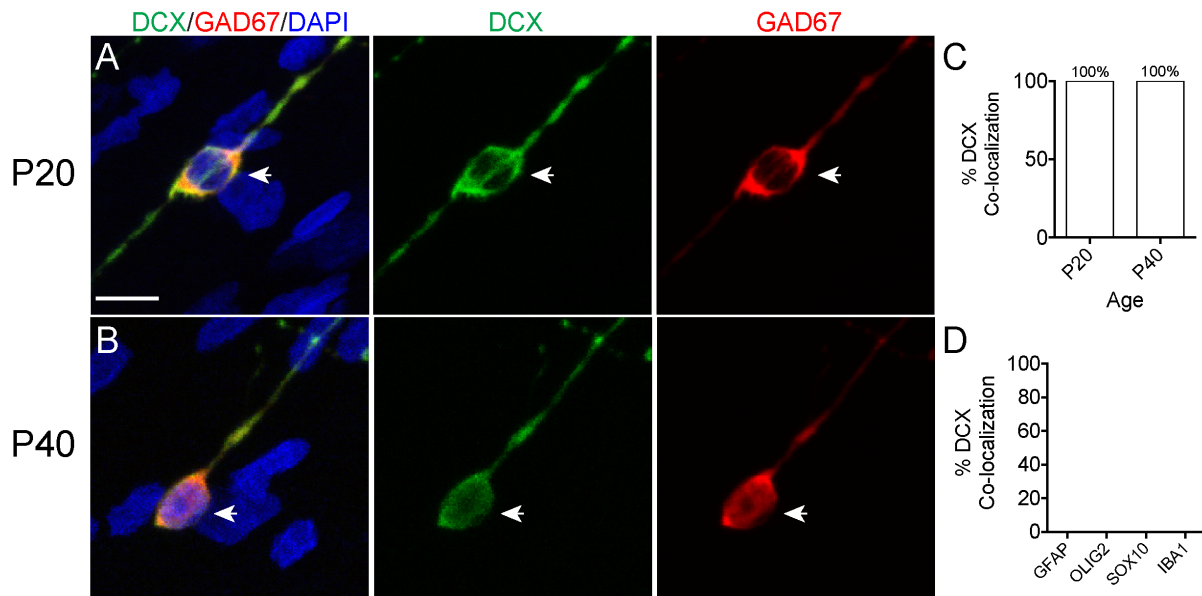
Figure 4.1. DCX+ cells express GAD67

DCX+ cells express GAD67 at P20 **(A)** and P40 **(B). C:** Quantification of %DCX co-localization with GAD67.
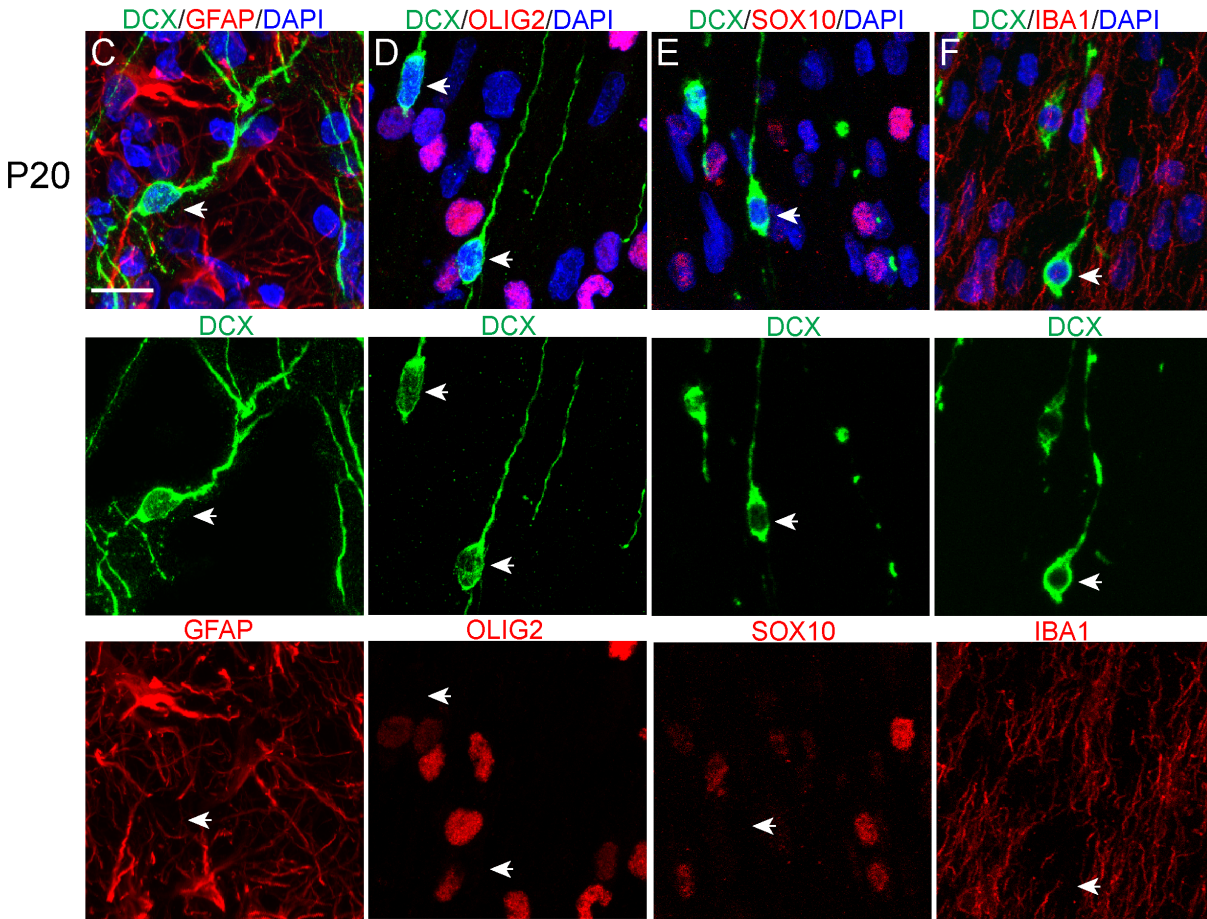
Figure 4.2. P20 DCX+ cells do not express glial markers

A: DCX+ cells do not express marker of astrocytes **B,C:** DCX+ cells do not express markers of oligodendrocytes. **D:** DCX+ cells do not express markers of microglia. Scale bar = 10um.

Next, I determined the percent co-localization for COUP-TFII in each stream at P20. The MMS had the highest percent co-localization at 76%. The DMS exhibited a 73% co-localization, and the PMS exhibited at 35% co-localization with DCX+ (**Fig. 4.3**).

As the majority of these cells expressed COUP-TFII, a marker of the caudal ganglionic eminence, I next stained P20 tissue for the markers Sp8 and Secretogogin (SCGN), both markers of interneurons originating in the CGE. SCGN+ cells co-localized with DCX 96% of the time in the MMS, 54% of the time in the DMS, and 83% of there time in the PMS (**Fig. 4.4**). Sp8+ cells co-localized with DCX 96% of the time in the MMS, 54% of the time in the DMS, and 82% of the time in the PMS (**Fig. 4.4**). This indicates that cells that are DCX/SCGN+ are also likely to be DCX/Sp8+. It also indicates that there may be multiple origins for these streams.

No DCX+ cells co-localized with Nkx2.1, a marker of the medial ganglionic eminence (**Fig. 4.5**). Furthermore, DCX+ cells at P20 did not express Somatostatin or Parvalbumin, interneuronal subtype markers of the MGE (**Fig. 4.5**). Finally,tTo determine if DCX+ cells expressed any markers of interneuron subtypes while in the white matter, I stained each stream Calretinin, Calbindin, NPY and VIP. No DCX+ cells co-localized with these markers in the white matter (data not shown).
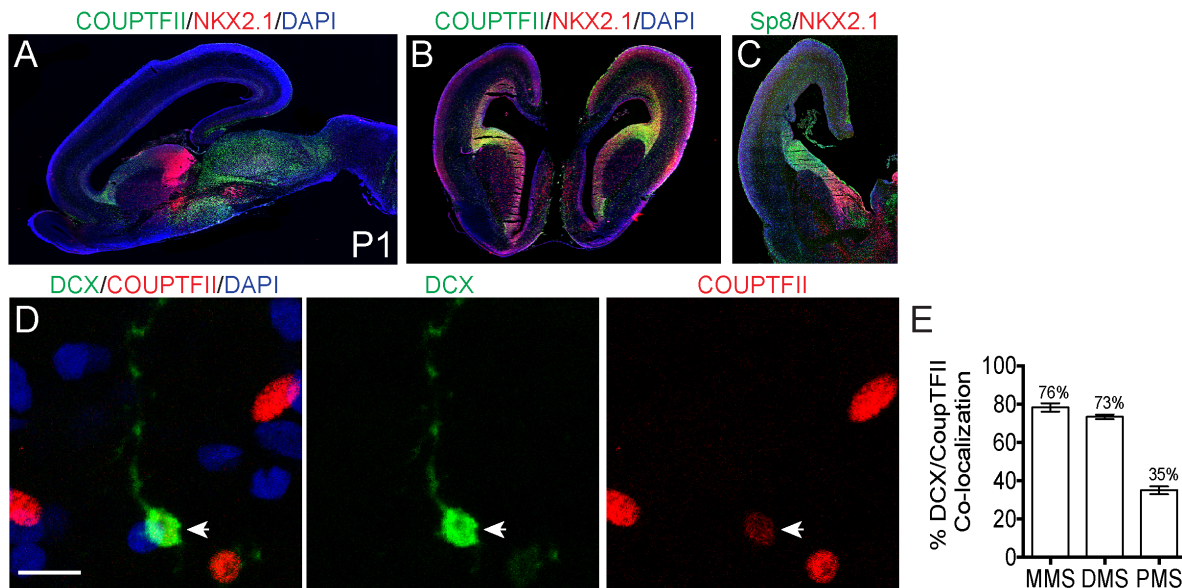
Figure 4.3. DCX+ cells express COUP-TFII

A: P1 sagittal ferret brain expresses COUP-TFII and Nkx2.1, markers of the CGE and MGE, respectively. **B:** Coronal section. **C:** Coronal section expressing Sp8 in the CGE and Nkx2.1 in the MGE. **D:** DCX+ cells express COUP-TFII. **E:** Percent co-localization of COUP-TFII and DCX in each stream. Scale bar = 10um.
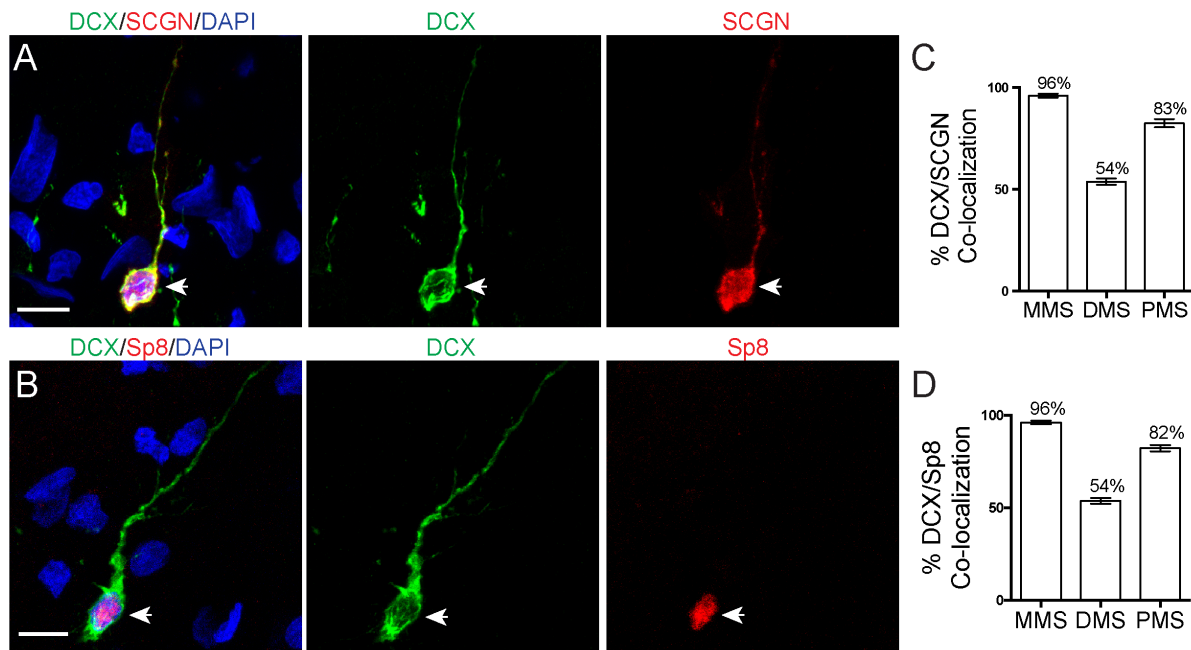
Figure 4.4. DCX+ cells express other Sp8 and SCGN

A: DCX+ cells express Sp8. **B:** DCX+ cells express SCGN **C,D:** Percent co-locaizations

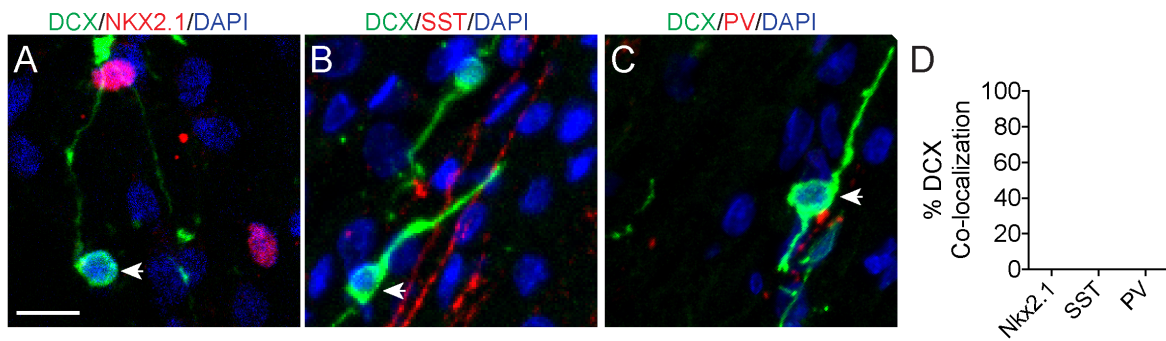of Sp8 and SCGN in each stream. Scale bar = 10um.

Figure 4.5. DCX+ cells do not express markers of MGE

A: DCX+ cells do not express Nkx2.1 **B:** DCX+ cells do not express Somatostatin. **C:** DCX+ cells do not express Parvalbumin. **D:** Quantification of percent DCX co-localization with MGE markers. Scale bar = 10um.

Chapter 5

The majority of doublecortin+ cells are observed transitioning from the white matter to the cortex

After discovering prominent streams of DCX+ young interneurons with a migratory morphology, I next wanted to understand the fate of these cells. As each stream dissipated over time, one possibility was that the cells were simply dying in the white matter. To investigate this possibility, I stained sagittal tissue at P20, P40, P65, and P90 with DCX and Cleaved Caspase 3, a marker of cells undergoing apoptosis. I then quantified the results, and to my surprise, the majority of Caspase+ cells appeared at P20 and then decreased over time. The least amount of Caspase+ cells were observed at P90 (**Fig. 5.1**). Therefore, the disappearance of the DCX+ cells between P40 and P90, depending on the stream, could not be explained by the cells dying.

While staining DCX+ cells for SCGN, I observed that some of the SCGN+ cells appeared to change their morphology in the white matter. No longer displaying the classic migratory morphology, these cells had mature looking, large cell bodies and multiple extended processes. These white matter interneurons did not co-localize with DCX (**Fig. 5.2**). In order to investigate if the majority of DCX+ cells transition into white matter dwelling SCGN+ interneurons, I stained sagittal tissue at P20, P40, P65, and P90 with DCX and SCGN and quantified the results. The number of SCGN+ white
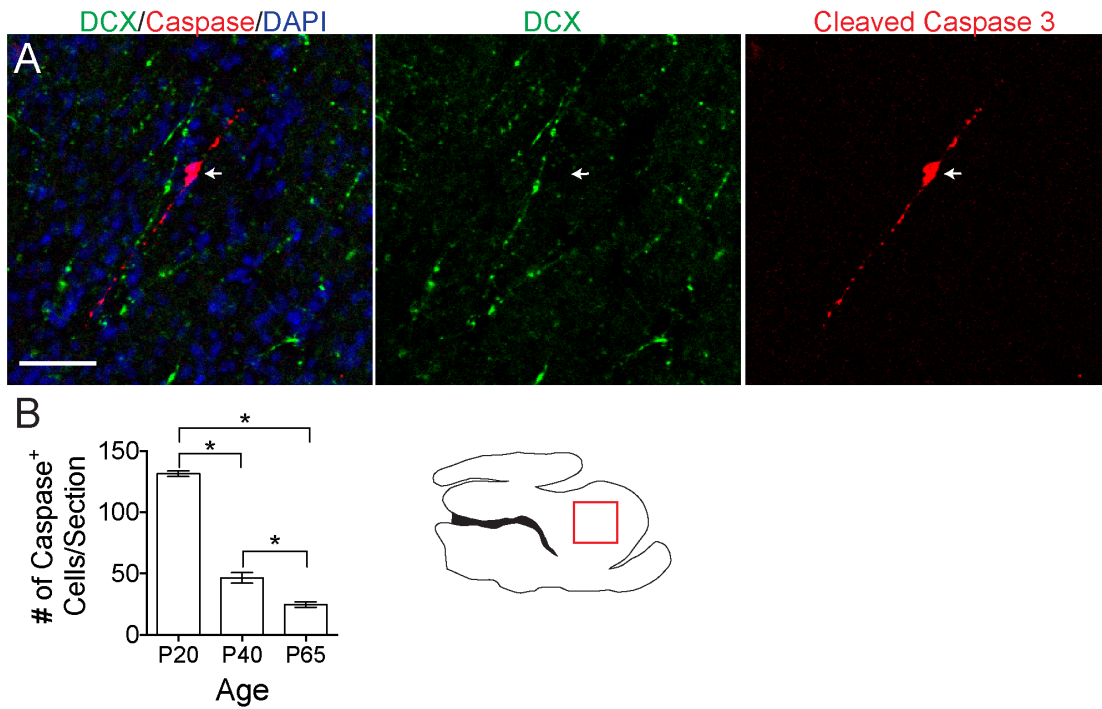
Figure 5.1. Number of caspase+ cells in the MMS decreases over time

A: DCX+ cell and cleaved caspase 3+ cell. **B:** Quantification of aspase+ cells in the
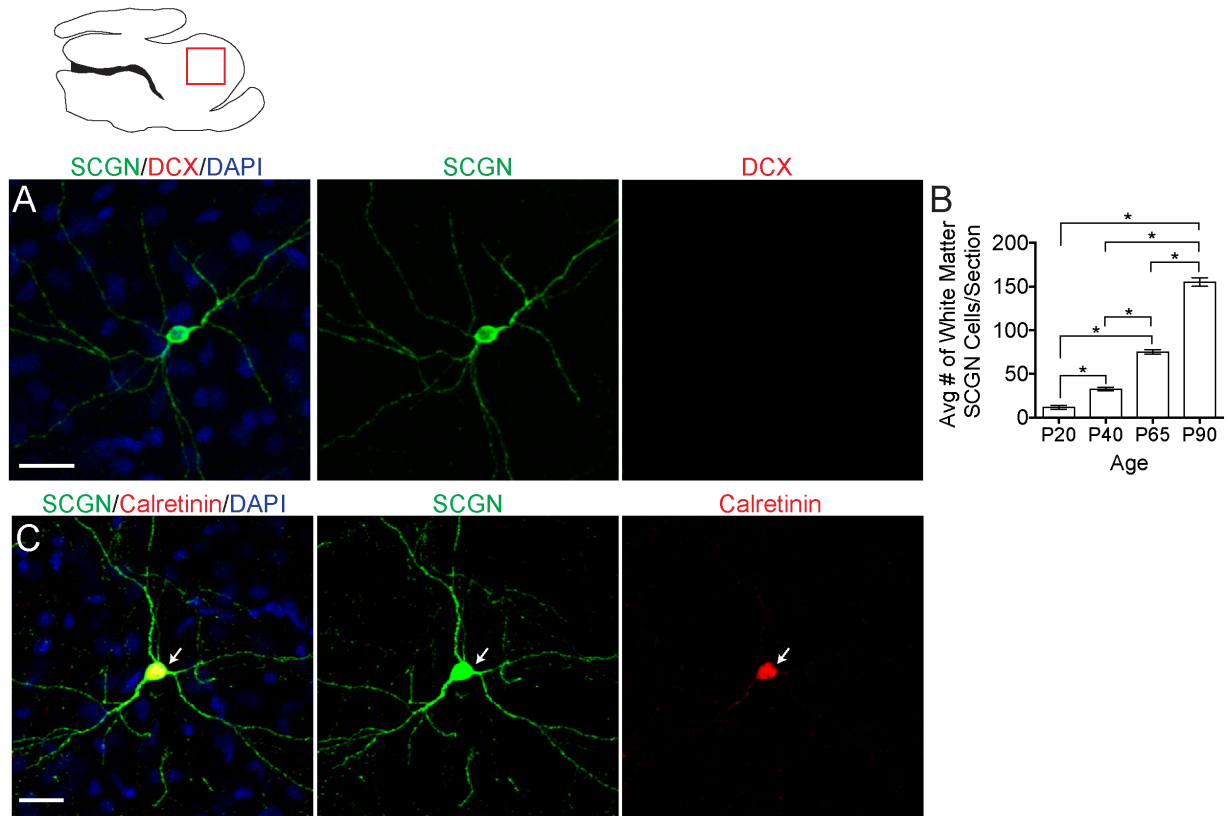
MMS over time. Scale bar = 10um.

Figure 5.2. SCGN+ cells mature in the white matter

A: Mature SCGN+ cell in the white matter of the MMS. **B:** Quantification of mature white

matter SCGN+ cells. **C:** White matter SCGN+ express Calretinin. Scale bar = 10um.

matter dwelling interneurons increased significantly with age. However, even then, the absolute number of white matter SCGN+ cells was significantly smaller than the accompanying number of DCX+ cells.

While staining for SCGN+ cells in the white matter, I observed several SCGN+ cells escaping the white matter and entering the cortex. If the majority of DCX+ cells are neither dying nor maturing in the white matter, then I would hypothesis that they are entering the cortex and contributing to circuit development. Re-examining the P20, P40, and P65 DCX/SCGN stained tissue, I observed the more SCGN+ cells appeared to transition into the cortex at P20, with fewer and fewer transitioning at P40 and P65 (**Fig. 5.3**).

In order to further explore whether or not the majority of SCGN+ cells at P20 were transitioning from the white matter into the cortex, I cleared P20 whole ferret hemispheres using IDISCO+. Once cleared and stained for SCGN, the hemispheres were imaged on a light sheet microscope in depths up to 5mm. By being able to appreciate millimeters of brain tissue at a time, I was able to appreciate the vast number of SCGN+ cells that appear to be transitioning into the cortex in both the coronal (**Fig. 5.4**) and sagittal (**Fig. 5.5**) planes. Spinning disk confocal microscopy allowed for higher magnification images to be taken, revealing that individual cells transitioning into the cortex possessed a migratory morphology. From these data, I concluded that the majority of DCX+ cells seen at P20 transitioned into the cortex.
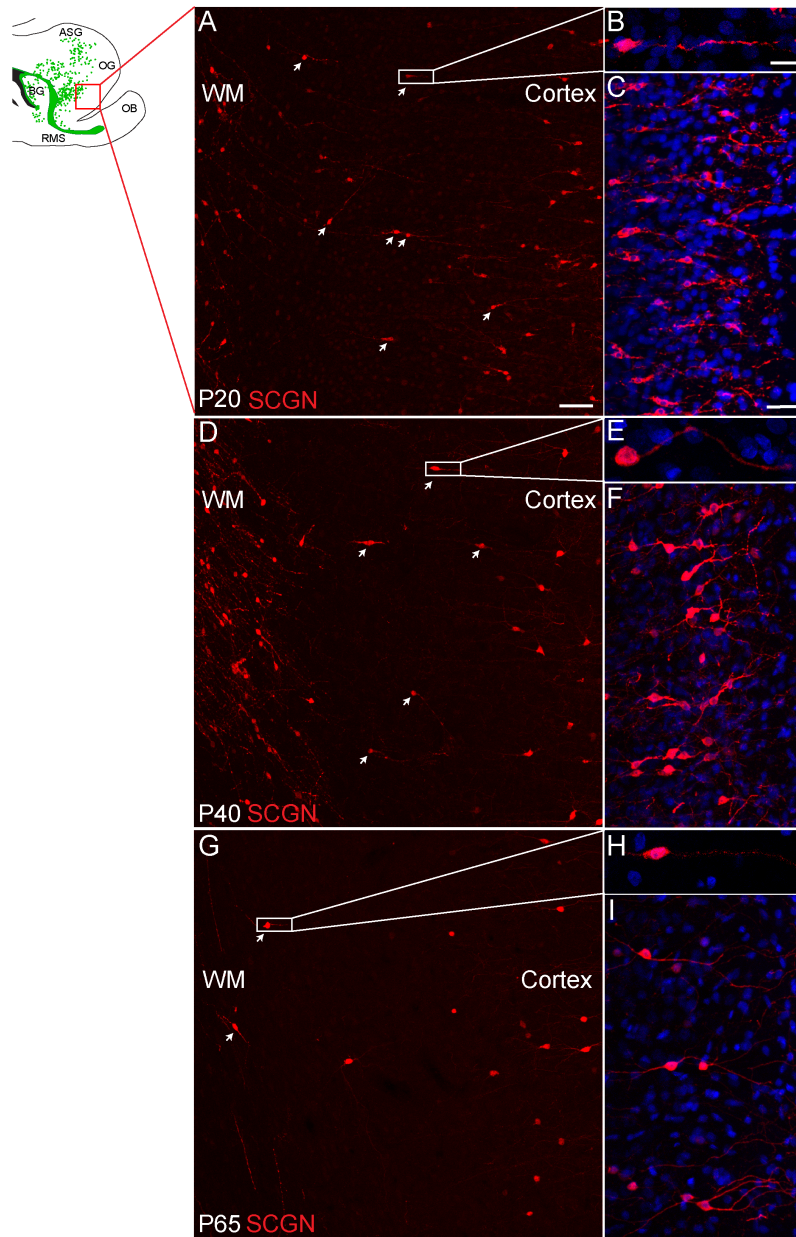
Figure 5.3. SCGN+ cells escape the white matter into the cortex

A: P20 MMS **B,C:** High mag pics of individual cell and cortex. **D:** P40 MMS **E,F:** High mag pics of individual cell and cortex. **G:** P65 MMS **H,I:** High mag pics of individual cell and cortex. Scale bar = 100um and 10um.
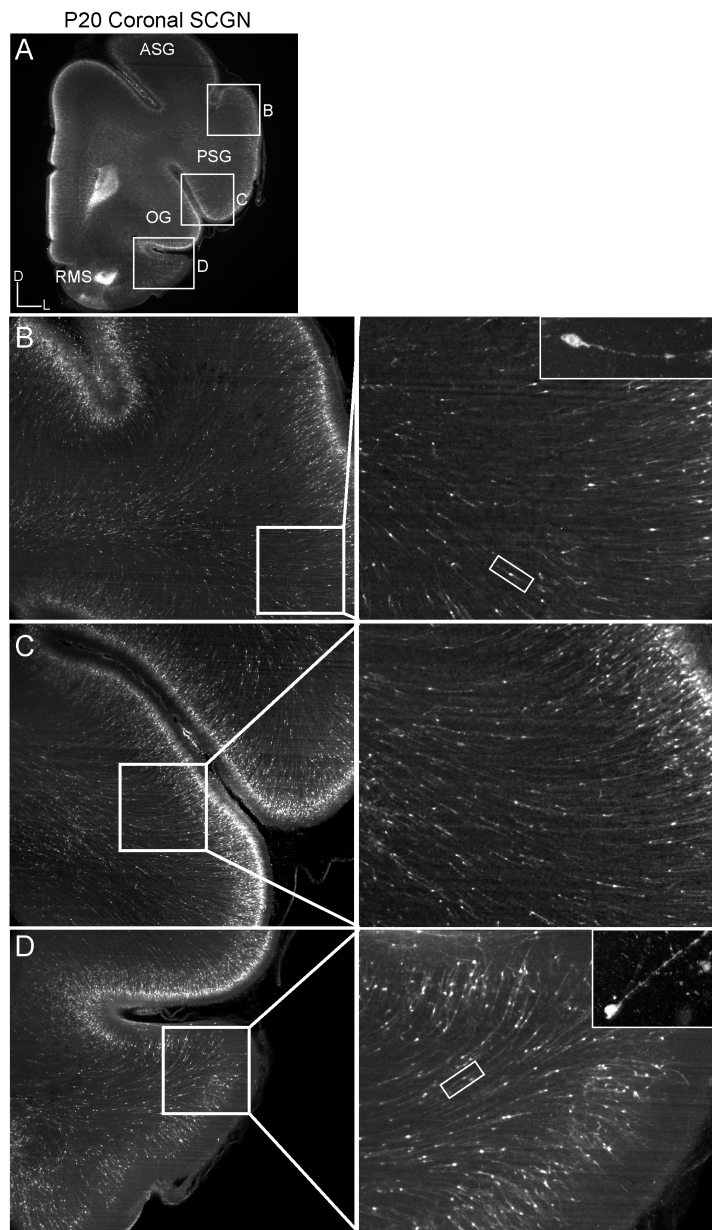
Figure 5.4. SCGN staining of iDISCO+ cleared P20 coronal hemisphere

iDISCO+ cleared brains reveal large populations of SCGN+ cells transitioning from the white matter into the cortex.
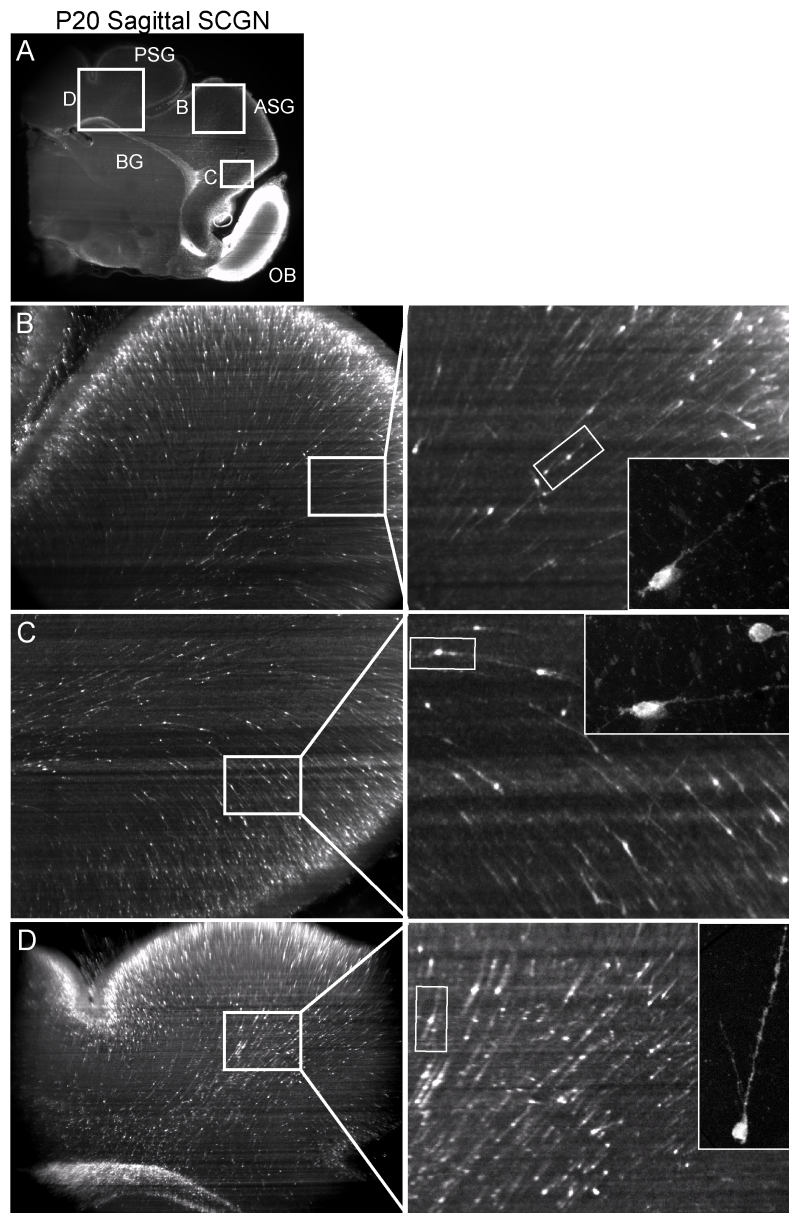
Figure 5.5. SCGN staining of iDISCO+ cleared P20 sagittal hemisphere

iDISCO+ cleared brains reveal large populations of SCGN+ cells transitioning from the

white matter into the cortex.

Chapter 6

Discussion

The major aim of my thesis was to investigate the existence of postnatal streams of interneurons in the ferret. My work showed that ferrets possess three robust postnatal streams of cortically oriented young interneurons.

Streams of young interneurons in postnatal ferret brain

The ferret has been used as a model for studying central nervous system (CNS) development for many years due to its gyrencephalic cortex and extended postnatal brain development. Because of these characteristics, ferret brain development is more similar to human and non-human primates than is rodent CNS development. My recent discovery that the postnatal ferret brain contains robust streams of young interneurons further strengthens this argument.

Ferrets possess three distinguishable streams of postnatal migrating interneurons. Ferrets contain a posterior stream of young interneurons that appears to originate at a bulge of doublecortin positive cells at the most caudal tip of the lateral ventricles. The stream is contained within the white matter and is oriented towards the occipital cortex. It continues to contain Dcx+ cells until postnatal day 40 and has disappeared by postnatal day 65. Caspase and secretogogin staining indicate that the majority of DCX+ cells neither die nor transition into mature neurons within the white

matter. This implies that young interneurons continue to contribute to occipital circuits until after P40. Ferrets don't usually open their eyes until P30. Therefore, the seeding of new interneurons may contribute to the opening of a critical period for vision. This would imply that these interneurons are important for development and not merely an afterthought. It is also important to note that as of yet, a posterior stream of interneurons has not been discovered in early postnatal human. Given the similarities between the other two ferret streams and known human streams, it seems likely that a human posterior stream of postnatal interneurons exists.

Ferrets also contain a dorsal stream of young interneurons that appears to originate at a bulge of Dcx+ cells surrounding the mid region of the lateral ventricles. The stream is contained within the white matter and is oriented radially towards the posterior sigmoid gyrus. The posterior sigmoid gyrus is a midline cortical structure thought to be equivalent to the human anterior cingulate gyrus, a region that is a part of the default mode network and is correlated with an individual's ability to mentalize. It was recently shown that the human ACC continued to receive migrating interneurons until the first six months of postnatal life. These interneurons differentiated into a variety of subtypes with the majority of them becoming neuropeptide Y positive. In the ferret brain, the young interneurons in the dorsal stream do not express subtype markers in the white matter, unlike human, so further work is needed to elucidate what subtypes they'll become.

Ferrets possess a medial migratory stream that branches off the RMS and contains young interneurons oriented towards the anterior sigmoid gyrus and the orbital gyrus, i.e. the ferret prefrontal cortex. This stream continues for quite a long period of

time, past P65, until disappearing by P90. Between P20 and P40, the stream condenses, and cells cluster together. All of these characteristics are similar to the reported MMS in humans. In humans, the MMS branches medially off the RMS and continues up until 9 months of age. It is oriented towards the ventromedial prefrontal cortex. It, too, goes from being a widely dispersed stream to condensed and full of Dcx/PSA-NCAM+ clusters.

Origins of young interneurons in postnatal ferret brain

Young interneurons in ferret postnatal streams express markers associated with the caudal ganglionic eminence. They express Sp8 and SCGN, two markers shown to be expressed in cells that originate in the CGE. A percentage of them also express Coup-TFII, a transcription factor found in cells that originate in the CGE. Young interneurons do not express markers or transcription factors associated with the medial ganglionic eminence, such as parvalbumin, somatostatin, or Nkx2.1. If these streams of interneurons are, in fact, born in the CGE, then that fits with what we know of CGE derived interneurons, namely, that they are late migrating, and that they are more likely to contribute cells to the upper layers of the cortex. In the mouse equivalency of the MMS, cells are positive for 5HT3a, another marker shown to be expressed in cells originating in the CGE.

If postnatal migrating interneurons are coming from the CGE in all three species, that raises several very interesting questions. First, why do stem cells in the CGE continue to proliferate for much longer than the MGE? Furthermore, for cells in the MMS at P65, when were they born? The CGE disappears a significantly long time before P65.

Destinations of young interneurons in postnatal ferret brain

In the human, the DMS and MMS appear to contribute interneurons to developing cortical circuits. The mouse, as well, appears to have an MMS that contributes calretinin positive cells to the lower layers of the orbitofrontal cortex. In the ferret, interneurons in postnatal streams are cortically oriented, and although they may not actually integrate into cortical circuitry, we show here that the majority of them do not mature and stay in the white matter, nor do they seem to undergo apoptosis. Furthermore, in 50um tissue sections, SCGN+ cells can be observed exiting the white matter and entering the cortex. Finally, iDISCO+ clearing of ferret brain hemispheres reveals a significant number of SCGN+ cells transitioning into the cortex. Therefore, we can hypothesize, in fact, that they do enter the cortex and integrate into developing circuitry. The continued addition of interneurons will undoubtedly affect the excitatory-inhibitory balance of those circuits. This raises interesting questions regarding the rules of integration. How do interneurons join circuits when there are only a few of them vs many? The extended postnatal development of the ferret CNS offers an excellent model to study interneuron integration into postnatal existing circuits.

Implications for circuit development and injury/disease

The perinatal and early postnatal time period is one of increased vulnerability to injury. Hypoxic injury during birth has been correlated with increased incidence of psychiatric disease later in life. Furthermore, traumatic birth injury in combination with several psychiatric risk single nucleotide polymorphisms has been correlated with an

increased risk of developing schizophrenia. In both human and ferret, robust streams of young interneurons are found in the early postnatal period, seemingly targeting different regions of the cortex. Furthermore, two of the regions targeted, the ventromedial prefrontal cortex and the anterior cingulate cortex, have been implicated in psychiatric disease. It is not unreasonable to hypothesize that injury during the perinatal and early postnatal period may affect these cells as they migrate. Their degree of vulnerability is currently unknown. However, in the mouse, some evidence exists that cells of the MMS are migrating along vasculature. If this is true in the ferret and human, then they may be dependent on high levels of oxygen to maintain their metabolism. Other factors, such as infection and stress, have been noted to affect brain development, and it would be very interesting to test the effect of these environmental factors on this model.

The human postnatal time period is characterized by rapid growth and the continued addition of interneurons to specific cortical regions. Like humans, ferrets have a gyrencephalic cortex and undergo extensive postnatal brain development. My thesis is the first to show that they also possess three robust postnatal streams of cortically oriented interneurons. Further investigation of this phenomenon may allow important questions of early postnatal cortical circuit development to be answered.

Chapter 7

References

1. Sanai N, Nguyen T, Ihrie R, Mirzadeh Z, Tsai HH, Wong M, Gupta N, Berger M, Huang E, Verdugo JM, Rowitch D, Alvarez-Buylla A. *Corridors of Migrating Interneurons in Human Brain and Their Decline During Infancy.* Nature. 2012; 478(7369): 382-386.

2. Paredes M, James D, Gil-Perotin S, Kim H, Cotter J, Nguyen C, Rowitch D, Xu D, Verdugo JM, Huang E, Alvarez-Buylla A. *Extensive Migration of Young Neurons into the Infant Human Frontal Lobe.* Science. 2016; 354(6308).

3. Inta D, Alfonso J, von Engelhardt J, Kreuzberg MM, Meyer AH, van Hooft JA, Monyer H. *Neurogenesis and Widespread Forebrain Migration of Distinct GABAergic Neurons from the Postnatal Ventricular Zone.* PNAS. 2008; 105(52): 20994-9.

4. Morton PD, Korotcova L, Lewis BK, Bhuvanendran S, Ramachandra SD, Zurakowski D, Zhang J, Mori S, Frank JA, Jonas RA, Gallo V, Ishibashi N. *Abnormal neurogenesis and cortical growth in hypoxia and disease.* Science Translational Medicine. 2017; 9(374).

5. McConnell SK. *Migration and differentiation of cerebral cortical neurons after transplantation into the brains of ferrets.* Science. 1985; 229(4719).

6. McConnell SK. *Fates of visual cortical neurons after isochronic and heterochronic transplantation.* Journal of Neuroscience. 1988; 8(3): 945-74.

7. Barnette A, Neil J, Kroenke CD, Griffith J, Epstein A, Bayly V, Knutsen A, Inder T. *Characterization of brain development in the ferret via magnetic resonance imaging.* Pediatric Research. 2009; 66(1): 80-84.

8. Duque A, McCormick D. *Circuit based localization of ferret prefrontal cortex.* Cerebral Cortex. 2010; 20:1020-1036.

9. Renier N, Adams E, Kirs C, Wu Z, Azevedo R, Kohl J, Autry A, Kadiri L, Venkataraju K, Zhou Y, Wang V, Tang C, Olsen O, Dulac C, Osten P, Tessier-Levigne M. *Mappaing of brain activity by automated volume analysis of immediate early genes.* Cell. 2016; 165: 1789-1802.

10. Renier N, Wu Z, Simon D, Yang J, Ariel P, Tessier-Levigne M. *iDISCO: A simple, rapid method to immunolabel large tissue samples for volume imaging.* Cell. 2014; 159: 896-910.

Publishing Agreement

It is the policy of the University to encourage the distribution of all theses, dissertations, and manuscripts. Copies of all UCSF theses, dissertations, and manuscripts will be routed to the library via the Graduate Division. The library will make all theses, dissertations, and manuscripts accessible to the public and will preserve these to the best of their abilities, in perpetuity.

Please sign the following statement:

I hereby grant permission to the Graduate Division of the University of California, San Francisco to release copies of my thesis, dissertation, or manuscript to the Campus Library to provide access and preservation, in whole or in part, in perpetuity.

_____   6/15/17
Author Signature   Date

51